Applied Energy 380 (2025) 125001

Contents lists available at ScienceDirect

Applied Energy

journal homepage: www.elsevier.com/locate/apenergy

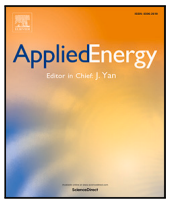

A comprehensive metric for resilience evaluation in electrical distribution systems under extreme conditions

Divyanshi Dwivedi [a,b,1], K. Victor Sam Moses Babu [a,c,1], Pradeep Kumar Yemula [b], Pratyush Chakraborty [c], Mayukha Pal [a,*]

[a] ABB Ability Innovation Center, Asea Brown Boveri Company, Hyderabad, 500084, Telangana, India
[b] Department of Electrical Engineering, Indian Institute of Technology, Hyderabad, 502205, Telangana, India
[c] Department of Electrical and Electronics Engineering, Birla Institute of Technology and Science, Pilani- Hyderabad Campus, Hyderabad, 500078, Telangana, India

ARTICLE INFO

Keywords:
Complex network
Energy resilient system
Critical loads
Resilience metrics
Distribution system planning
Distributed energy resources
Automated switches

ABSTRACT

Due to the increasing occurrence of extreme weather events and cyber threats in electrical distribution systems (EDS), it is of paramount importance that power system planning and operations develop and enhance the system's resilience. Several researchers have proposed various resilience metrics, but a comprehensive metric is still necessary that integrates multiple dimensions of resilience, such as robustness, adaptability, and recovery, which are specific to the characteristics of EDS. This paper proposes a novel framework for resilience evaluation with a holistic metric that takes into consideration both the topological constructs from complex network parameters and the electrical service requirements. The proposed metric follows the resilience analysis process, a risk-based decision-making technique that contains six steps for assessing system performance. The resilience evaluation facilitates a quantitative analysis that evaluates the impact of control decisions, providing a proactive and resilient operation of distribution systems. A systematic approach for the enhancement of resilience in EDS is proposed by efficiently integrating distributed energy resources (DERs) and automated switches, resulting in high resilience scores above 90%. To demonstrate the performance of the proposed methodology, the algorithm is applied to a modified IEEE 123 node test feeder and tested for various cases of DER integration and additional switches, increasing the system resilience from 56% to 93%. The proposed framework effectively selects the most resilient network configuration under an extreme event for initial service restoration, increasing the resilience of the system from 2% to 23% depending on the extent of damage to the infrastructure and availability of resources. This quantifiable metric proves to be a valuable tool for resilience-based planning and operation.

1. Introduction

To fulfill the demands of consumers, utilities, and society, electrical distribution systems are required to be reliable and resilient. Uninterrupted and consistent power supply is essential for various crucial loads, including industrial production, fire stations, national security, trade, public transportation, hospital operations, and communication. However, the increasing frequency of events that cause severe natural disasters has exposed vulnerabilities in the EDS [1]. The occurrence of power disruptions that are triggered by severe weather conditions leads to substantial economic setbacks, poses threats to public safety, and disrupts essential services. This work aims to tackle the important task of strengthening the EDS to guarantee a continuous power supply during disruptive events [2].

Natural disasters, like storms and hurricanes, seriously threaten power systems, causing extensive damage and prolonged outages. For example, hurricane Sandy in 2012 affected 4.2 million customers who faced a 10-day power outage, and Hurricane Maria in 2017 affected 3.6 million residents in Puerto Rico [3]. In 2020, the United States experienced a record-breaking year for power outages, as revealed by an analysis from the Energy Information Administration (EIA) [4]. As of 2021, the trend continues, with hurricane Ida causing power losses for 1.2 million customers across eight states and a sudden cold snap in Texas in February affecting over 4.5 million customers. In November 2023, Storm Ciarán left over a million people in France without electricity, highlighting the critical need for enhanced resilience in power systems [5]. It affected France, the Channel Islands, and southern

* Corresponding author.
E-mail address: mayukha.pal@in.abb.com (M. Pal).
[1] Authors contributed equally.

https://doi.org/10.1016/j.apenergy.2024.125001
Received 8 April 2024; Received in revised form 29 October 2024; Accepted 22 November 2024
Available online 6 December 2024

England, leaving over a million people without electricity. France's northwest department of Finistère was affected the most, where winds exceeded 120 kph (75 mph) and gusts surpassed 200 kph (124 mph), resulting in power outages for 1.2 million people. The northwestern region of Brittany faced the brunt, with 780,000 affected individuals, while the southwestern county of Cornwall recorded 8,500 people without power.

In the summer of 2010–2011, Queensland, Australia, faced extensive flooding, causing significant damage to six zone substations, as well as numerous utility poles, transformers, and overhead cables [6]. This, in turn, resulted in electricity disruptions for approximately 150,000 consumers. During January 2023, California faced rounds of heavy rain, wind, and snow, leading to flood alerts and power outages affecting more than 19,000 customers [7]. In August 2023, heavy rain in Ottawa, Canada, resulted in approximately 24,000 customers losing power. Within three hours, the situation improved, with estimates indicating that fewer than 1,000 customers remained without power [8]. Following the heavy rain, Hydro Ottawa deployed about 225 work crews to restore power to those affected and address over 725 different outages. Although the restoration process is generally a multi-day effort, they managed to significantly reduce the number of customers without power within three hours. The quick recovery is attributed to Hydro Ottawa's efficient detection and restoration process, which includes assessing the damage, repairing main transmission lines and substations, and then addressing local lines to homes and businesses. Extensive losses have been experienced from the wildfire events where severe wildfires engulfed California in early September 2020, wreaking havoc on the state's solar power production and causing a substantial drop of nearly one-third in solar generation. As the state is heavily dependent on solar installations for almost 20 percent of its electricity, this caused a significant setback [9].

Such incidents have a severe impact on energy infrastructure, resulting in significant challenges in maintaining electricity supply. These examples highlight not just the vulnerability of power systems to natural disasters but also the critical difference between reliability and resilience in EDS [10]. Reliability refers to the ability of the electrical grid to deliver power continuously under normal operational conditions, while resilience is about the grid's ability to prepare for, respond to, adapt, and recover from adverse events that cause disruptions. In the face of extreme events, enhancing resilience means strengthening not only infrastructure against potential damages but also quick restoration capabilities, as demonstrated by Hydro Ottawa's rapid response following heavy rains. Building resilient power systems involves strategic planning, robust construction, and adaptive operational practices that can mitigate the impact of these disruptions, thereby ensuring a more secure and stable power supply in increasingly uncertain environmental conditions.

2. Power grid resilience

2.1. Background of resilience

Resilience was initially introduced by C.S. Holling in 1973 as a measure of how well a system endures and adapts to changes and disruptions with its interactions between populations or state variables [11]. In 2002, Lachs worked to restore and protect the stability of the power grid during challenging events [12]. From 2000 to 2016, most of the research emphasized in improving the reliability of the power grid. However, in comparison to reliability, the exploration of resilience is still in its initial phases. Despite the presence of multiple definitions, establishing a universally accepted one remains a challenge. The scope of resilience includes risk assessment, anticipation, adaptability, reliability, recovery, and robustness, as it is crucial to acknowledge events with low probability but high potential impact.

Another more systematic understanding of the stages concerning resilient operations and the resilience trapezoid has been investigated [13,14]. The resilience trapezoid, illustrated in Fig. 1, offers a detailed examination of the resilience state when facing disruptive events. A resilient system has capabilities to prevent, absorb, recover, adapt, and resist, which shows how a system responds to an extreme event with minimal disruptions in its operations. The goal is not only to bring the system back to its initial operational state but also to make sure it becomes less susceptible to similar occurring events [15]. Additionally, Fig. 1 illustrates a pair of curves that evaluate system performance, one based on the infrastructure properties and the other on the service delivered to critical loads. The proposed metric synthesizes these two perspectives, resulting in a robust resilience assessment tool for EDS. This combined metric takes into account not only the critical load demand but also the physical robustness of the network, offering a holistic evaluation of an EDS's resilience.

In 2022, the IEEE task force proposed a comprehensive definition of power system resilience aimed at capturing the essence of the grid's ability to endure and respond to adverse circumstances. The definition [15] is as follows: "Power system resilience is the ability to limit the extent, system impact, and duration of degradation in order to sustain critical services following an extraordinary event. Key enablers for a resilient response include the capability to anticipate, absorb, rapidly recover from, adapt to, and learn from such an event. Extraordinary events for the power system may be caused by natural threats, accidents, equipment failures, and deliberate physical or cyber-attacks."

This definition highlights the power grid's ability to endure and bounce back from exceptional events, covering natural threats, accidents, equipment failures, and intentional attacks. It aims to provide uninterrupted supply to critical loads like national security, industrial production, hospital operations, public transportation, and communication networks. This work used the above-mentioned definition for the evaluation of the resilience of the power distribution system. It is characterized by the network's capability to withstand interruptions in power supply to critical loads (CLs) during challenging operating conditions and its ability to recover from any damages incurred during adverse events.

Extensive work has been done to justify control strategies, algorithms, and actions in the distribution management system when responding to extreme events. Various resilience metrics have been proposed to quantify the feasibility of planning decisions [16–21]. However, existing metrics do not follow the resilience analysis process (RAP) outlined by Sandia National Laboratories [22]. The RAP encompasses six primary steps for assessing system performance, as shown in Fig. 2, providing a structured methodology for improving critical system resilience and guiding investment strategies. In addition to these steps, the resilience metric needs to be useful, comparable, applicable across operations and planning, applicable and scalable, quantitative and qualitative, incorporate uncertainty, consider a risk-based approach, and consider recovery time [22].

2.2. Literature review

2.2.1. Existing resilience metrics

Traditionally, the evaluation of an EDS performance over an extended period relies on reliability metrics such as system average interruption duration index (SAIDI), system average interruption frequency index (SAIFI), and momentary average interruption frequency index (MAIFI) [2], which are designed to measure how effectively the system delivers power to all connected loads. However, in extreme adversity, prioritizing power supply to critical loads before addressing non-critical ones becomes crucial [17,18]. This capacity of the system to ensure uninterrupted power supply to critical loads during severe and unfavorable events is referred to as "resilience" and adequately assessed using traditional reliability metrics [16]. However, numerous quantifiable metrics for network resilience estimation have been proposed in the literature [23–25]. In [1], a resilience metric was proposed that includes topology-based and feasible-network-based parameters, but it does not account for all possible paths available to supply critical

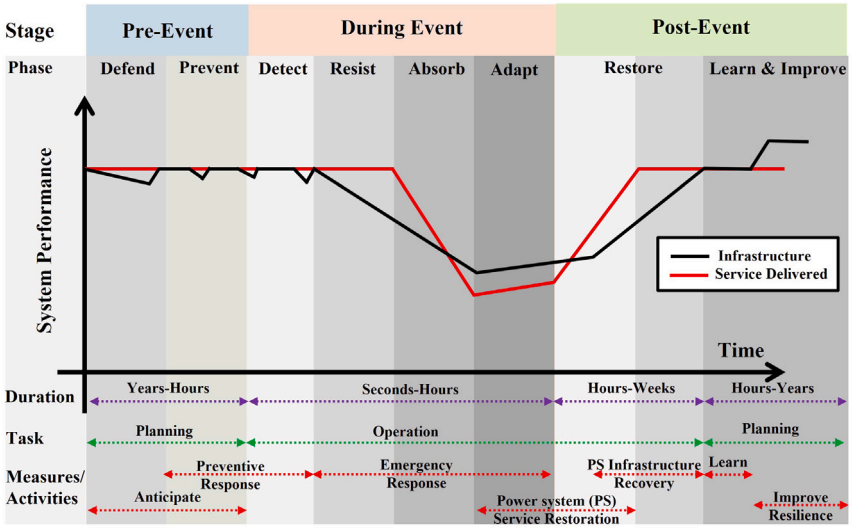

Fig. 1. Typical curve for system response to an extreme event [15].

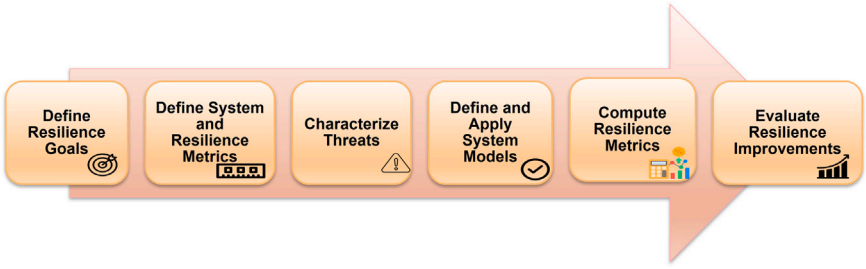

Fig. 2. Illustrates the sequential stages of the RAP [22].

loads during extreme events. Another method is proposed to quantify the resilience of a power distribution system using percolation theory and complex network analysis [21]; the resilience is estimated based on topological network, the failure rate of network equipment, power flow feasibility, and intensity of a threat.

A quantitative model and metric for the resilience of EDS is developed [24]; availability is considered a basic measure, and brittleness and resistance are defined as key resilience-related principles. Also, a real-time resilience framework based on the analytical hierarchy process is used for the analysis and design of energy storage with different power-to-energy ratios [17]. Resilience computation involves representing the power system as a graph and computing graph-theoretic parameters such as the fraction of damaged nodes, algebraic connectivity, graph diameter, characteristic, betweenness centrality, and redundancy coefficient [17]. Graph-based models may assume a certain level of homogeneity in the power system, treating all nodes and components equally.

In reality, there may be variations in the criticality of different components, and their resilience may vary. Failing to account for this heterogeneity could lead to inaccurate resilience assessments. Other proposed metrics include branch count effect, overlapping branches, switching operations, repetition of sources, path redundancy, and probability of availability and penalty factor [25]. A resilience framework, named anticipate, withstand, and recover (AWR), is formulated for monitoring system resiliency [19]. The framework is designed to be applicable before, during, and after extreme events, covering the entire event progression. A conceptual resilience curve is presented, illustrating the expected outcomes of the proposed AWR metrics, including delayed impact, reduced impact, enhanced recovery performance, and better post-event performance. Factors impacting resilience are identified based on system characteristics and attributes at each stage of event progression. However, formulation and implementation of this resilience framework could introduce complexity, pose challenges during the implementation phase, and require significant resources and expertise.

A quantitative comparison of each resilience metric is limited due to intrinsic differences in their design, scope, and focus areas. However, to the best of scope, Tables 1 and 2 provide a detailed comparison of the proposed resilience metric with existing metrics. These metrics often rely on different units of measurement or scales, making direct numerical comparison unfeasible. Metrics M1, M3, M4, M5, M6, and M7 are unitless and fall within the range of [0,1] for M1, M4, M6, and M7. Similarly, for M2, M3, and M5, the minimum value for the resilience score is zero, and they do not have an absolute upper bound within the formula itself but are limited by the power constraints of the network. Therefore, a direct quantitative comparison is constrained. Thus, Tables 1 and 2 provide a detailed comparison of resilience metrics in the prior art with our proposed metric, covering all aspects and dimensions of resilience. This comparison allows for a better assessment of the evaluation criteria and considerations of each resilience metric in the distribution system, providing an overview of each metric's strengths and limitations, as detailed in Table 2. Each of these metrics evaluates distinct aspects of resilience, such as operational and planning dimensions, and uses different topological and electrical service parameters. None of the aforementioned metrics in the prior art have followed the detailed steps set forth in the RAP and IEEE task force definition and framework. While some aspects of resilience evaluation have been explored in previous works like M7, this paper presents the first metric that comprehensively aligns with both RAP and IEEE Task Force frameworks. This alignment represents a significant advancement as it requires integrating parameters that meet all framework requirements across different event stages while maintaining consistent evaluation capabilities.

Table 1
Comparison of various resilience metrics and evaluation process.

Reference	Resilience metric	Evaluation process	Range	Remarks
M1 [21]	The resilience metric $\Re$ consists of 6 complex network-based parameters	AHP is used to compute a composite resilience score. Two-stage reconfiguration algorithm optimizing network responses to disruptions.	Min - 0 Max - 1	Evaluates resilience based on topological resilience to maintain service continuity by strategically adapting the network layout.
M2 [26]	$\Re = \int_{t_d}^{t_r^*} \sum_{c \in C} w_c \cdot p_c(t)\, dt$ t_d: restorative state, t_r^*: post-restoration state, C: set of critical load, w_c: weight of a critical load, $p_c(t)$: active power of load c at time t	Stochastic post-hurricane framework for resilience enhancement using mobile emergency resources and pre-hurricane resource allocation.	Min - 0 Max - Depends on system constraints	A stochastic, energy-based, and operational resilience metric to evaluate the system's ability to restore critical loads in micro- grids.
M3 [27]	$Re_{i,j} = \frac{P_i^{\max} - P_{i,j}}{P_i^{\max}}$ $Re_{i,j}$ is the resilience index for the ith operational temporal period and the jth failure mode, $P_i^{\max}$: penalty cost if all functional services are lost, and $P_{i,j}$: penalty cost of lost functional services.	A loss matrix captures service failures and assigns penalty costs, forming a normalized resilience matrix where lower values indicate higher resilience.	Min - 0 Max - Depends on system constraints	Normalizes the imposed costs to quantify the resilience index, providing a comprehensive measure of system resilience under various scenarios.
M4 [25]	Resilience is computed via the Choquet Integral using resilience parameters consisting of 2 complex network-based parameters and 5 operational and structural parameters.	Compute the Choquet integral by aggregating parameters considering weights and interactions.	Min - 0 Max - 1	Captures the system's robustness and adaptability, accounting for the complex interplay among various resilience factors.
M5 [28]	$R_j = \frac{\alpha_1 \cdot \mathrm{bc}_j}{\alpha_2 \cdot \frac{d_{g,j}}{d_{\max}}} \times \frac{P_{\text{critical}}}{P_j}$ α_1, α_2: weights, bc_j: betweenness centrality, $d_{g,j}$: geodesic path length, $d_{\max}$: maximum path length, P_{critical}: critical load demand, P_j: total load	An algorithm uses D-PMU data to monitor bus angular differences, classify feeders at risk, and compute R_j for optimal reconfigurations.	Min - 0 Max - Depends on system constraints	Real-time adjustments are made based on updated data for dynamic adaptation to extreme events and maintain power supply to critical loads.
M6 [1]	Topology-based resilience metric, $\Re_T$ which consists of 8 complex network parameters. Feasible network-based resilience metric, $\Re_{FN}$ consists of 2 complex network parameters and 6 operational & service parameters	AHP is used to compute resilience scores for different network configurations, ensuring a continuous supply to critical loads during and after disruptions.	Min - 0 Max - 1	These sets of metrics facilitate a multifaceted assessment of a system's robustness and adaptability to disruptions, considering both the topological structure and the operational capabilities.
M7 [19]	Three individual resilience metrics are used with different parameters for anticipation, withstanding, and recovery.	AWR framework integrates system characteristics before, during, and after extreme events to compute resilience scores for operational and planning decisions in the EDS.	Min - 0 Max - 1	Factors impacting resilience are identified based on system characteristics and attributes at each stage of event progression.

Table 2
Qualitative comparison of resilience metrics.

Reference	Year	Electrical parameters	Topological parameters	Operational metrics	Planning metrics	Considers RAP	Enhancement methods	Contingency analysis	Critical load analysis	Considers IEEE task force framework
M1 [21]	2016	–	Yes	Yes	Yes	–	–	–	Yes	–
M2 [26]	2016	Yes	–	Yes	–	–	Yes	Yes	Yes	–
M3 [27]	2018	Yes	–	Yes	–	–	Yes	–	Yes	–
M4 [25]	2018	Yes	–	Yes	Yes	–	Yes	–	Yes	–
M5 [28]	2020	Yes	Yes	Yes	–	–	–	Yes	Yes	–
M6 [1]	2021	Yes	Yes	Yes	Yes	–	Yes	Yes	Yes	–
M7 [19]	2022	Yes	Yes	Yes	Yes	–	Yes	Yes	Yes	–
Proposed Metric	**2024**	**Yes**	**Yes**	**Yes**	**Yes**	**Yes**	**Yes**	**Yes**	**Yes**	**Yes**

As resilience enhancement is a key feature of RAP, this work focuses on enhancement strategies in EDS. In M6, some of the considered cases for resilience enhancement are similar to those in this work, such as the integration of distributed energy resources (DERs) and the use of additional switches. Consequently, the quantitative comparison of these similar cases is discussed in detail in Section 6. On the other hand, resilience enhancement in M2 was achieved using mobile emergency resources; M7 utilized battery storage systems; M3 employed solar PV systems; and M4 focused solely on additional switches without DERs.

Comparisons with these metrics could not be performed because the considered systems and case scenarios differ. In this work, the considered contingency cases are similar to two scenarios (hurricane and short-circuit fault) in M6; however, since composite resilience scores are not computed in M6, a direct comparison could not be made. The contingency cases in M2, M5, and M7 differ from those in the current work and pertain to different systems, preventing any direct comparison of contingency cases. Therefore, in this work, quantitative comparisons with M6 are made for a few case scenarios of resilience

enhancement. However, M6 does not encompass the features included in the proposed metric, such as alignment with RAP and the IEEE task force definition and framework. The proposed metric in this work integrates all the specified dimensions, such as the inclusion of electrical service parameters, topological considerations, operational and planning metrics, adherence to the RAP standard, and alignment with the IEEE task force definition and framework, indicating its comprehensive nature in assessing resilience in EDS compared to other resilience metrics in the literature.

2.2.2. Strategies for resilience enhancement

Various planning and operational techniques are employed to improve the system's capacity to withstand and recover from diverse disruptions or adversities. These techniques are designed to improve the system's ability to adapt, absorb shocks, and persist in operation under challenging conditions. Distributed energy resources play a crucial role in enhancing system reliability, mitigating the impact of blackouts, and optimizing power distribution [29,30]. As the integration of distributed generation (DG) continues to grow within centralized electricity systems, it becomes imperative for utilities to strategically allocate DG to enhance the voltage profile, reform reliability, and minimize losses [31,32]. Numerous scientific papers have explored distribution system expansion planning strategies involving DERs, each proposing distinct approaches to achieve optimal DER allocation. Researchers have placed emphasis on minimizing power and energy losses [33,34], managing schedulable and intermittent power generation patterns [35], and reducing DG-related investment and network maintenance costs [36]. Another strategy involves the optimal allocation of diverse DG technologies and the formation of microgrids within the EDS to enhance reliability and supply security [37]. As the life of lithium-ion batteries is improved through AI techniques [38,39], fixed storage [40,41] and mobile storage [42,43] would also help in resilience enhancement.

Additionally, the strategic placement of automated tie-line switches is vital to enhance resilience by expanding the number of possible restoration paths during disturbances. These switches swiftly isolate faulted areas within the distribution system, redirecting power flow to maintain service. While previous studies have addressed switch placement focusing on reliability satisfaction [44,45], we introduce a systematic approach to EDS planning centered on resilience performance. The study provides insights into the integration of DERs and the installation of automated switches from a resilience perspective, aiming to improve the system's ability to anticipate, withstand, and recover from adverse events.

2.3. Main contributions and paper organization

The objective of the paper is to help operators in resilience evaluation and metrics-based decision-making to maximize the resilience of the power distribution system and develop a resilience metric to quantify resilience. The key contributions of the work are as follows:

1. A comprehensive resilience metric is proposed that quantitatively measures and evaluates the resilience of EDS for different infrastructure modifications of the system, such as integration of DERs and operation of additional switches.
2. The proposed metric has three electrical parameters that indicate a quantitative assessment of the EDS through (i) service fulfillment, (ii) number of possibilities to fulfill the service requirement, and (iii) the ability to meet additional services. To provide a qualitative assessment of the physical properties of the EDS infrastructure, two complex network parameters are used to indicate (i) topological strength determination through an edge removal process and (ii) efficiency computation of important nodes in the system through a node removal process.
3. The proposed resilience metric is evaluated for various contingency events such as flood, wildfire, hurricane, and short-circuit faults where the resilience of the system is observed through the resilience curve in terms of both service requirements and physical properties of the infrastructure.
4. The proposed metric is in line with the IEEE task force definition of resilience and also encompasses all crucial elements of the resilience metric that are required by the RAP provided by Sandia National Laboratories, indicating the robustness and comprehensiveness of the proposed methodology.
5. A systematic approach is proposed to enhance resilience by efficiently integrating DERs and automated switches into EDS.

The paper is structured as follows: Section 3 details a comprehensive framework for evaluating the resilience of EDS, focusing on topological characteristics and critical load serving. Section 4 provides a step-by-step methodology for applying the proposed metric to assess network resilience and provides details about the test model. In Section 5, simulation results demonstrate the effectiveness of the framework in evaluating existing network resilience, as well as its ability to quantify the impact of additional switches and the integration of DERs. Furthermore, case studies involving extreme events, including floods, wildfires, hurricanes, and fault events, illustrate the framework's applicability across diverse scenarios are discussed in Section 6. The paper concludes by summarizing key findings, discussing broader implications, and suggesting potential directions for future research in the field of power distribution network resilience in Section 7.

3. Proposed resilience metric

3.1. Considered system

For analysis, the IEEE 123 node test feeder is considered, as shown in Fig. 3. The system operates at a nominal voltage of 4.16 kV, with the main substation node (node 150) having a rated power supply of 5000 kVA. The total load demand is 3855.26 kV spread across 85 load nodes of the distribution system. The key feature of the IEEE 123 node test feeder is the availability of switches (6 closed switches and 6 open switches) that could be operated under an extreme event, providing alternate paths for supplying to the critical loads. Thus, the multifaceted nature of the IEEE 123 system provides a realistic model for testing and analyzing the distribution system for different switching operations under various contingency events. The system is modified by adding four distributed energy resources placed at nodes 49, 21, 105, and 56 with a rating of 350.35 kVA each. The integration of these DERs would help in enhancing the system's resilience. The critical loads in an EDS are generally essential services, and their locations are known and predefined to the distribution system operators for efficient resilience operation. We have considered two critical loads that have the maximum load demand in the EDS to have an assessment of the power delivered to these loads from all available sources during extreme events. According to the details provided in [46], it is evident that nodes 48 and 76 exhibit a high load requirement of 258.20 kVA and 303.69 kVA, respectively. These nodes are considered critical because they account for a combined load demand of 561.89 kVA, which is 15% of the total load demand (3855.26 kVA) of the entire EDS. These critical loads (CLs) serve essential facilities such as hospitals and data centers, requiring a continuous and uninterrupted power supply during unforeseen extreme events. Thus, these nodes are considered critical, necessitating their need for a continuous and uninterrupted power supply during unforeseen extreme events. These critical loads serve essential facilities such as hospitals, data centers, etc.

The proposed metric for resilience evaluation considers (i) electrical service requirements by considering the available possible paths to supply power to critical loads, the percentage of critical loads met,

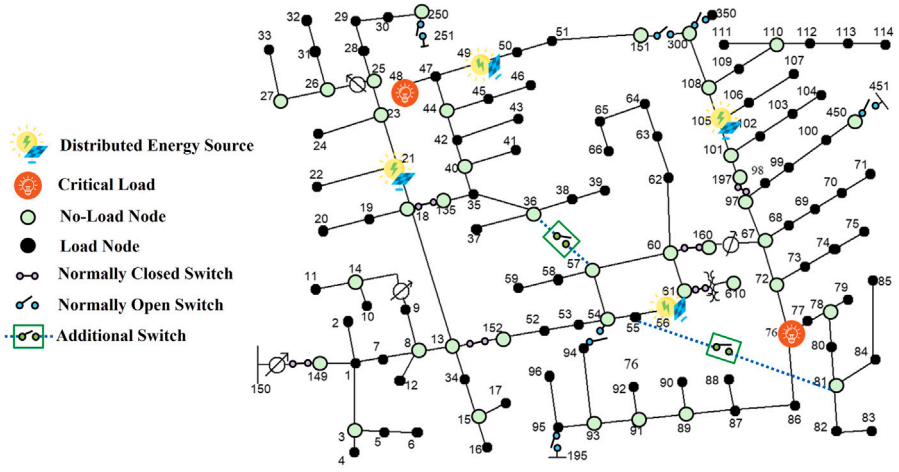

Fig. 3. Single line diagram of IEEE 123 node test feeder, with integration of additional switches and DERs.

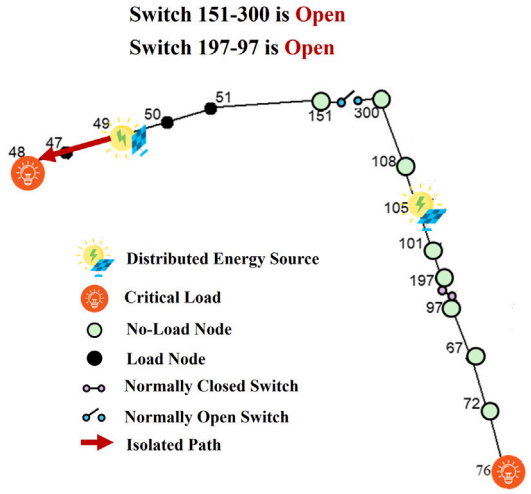

Fig. 4. Isolated path from one source to one critical load.

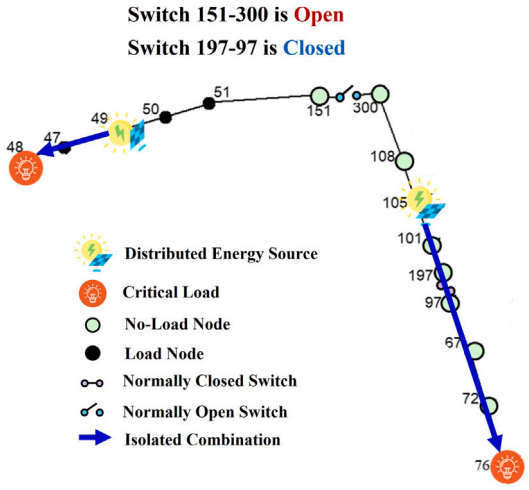

Fig. 5. Isolated combination from two separate sources to two different critical loads.

and the energy supply available to meet the load demand, and (ii) topological network strength using two key parameters derived from the concepts of complex network theory. By combining these parameters, a comprehensive evaluation of the EDS's resilience is performed by considering not only the physical robustness of the network but also its ability to meet critical load demands during disruptions.

3.2. Parameters for electrical service requirements

3.2.1. Weighted path variability

In this study, the resilience of EDS is evaluated in terms of the availability of power supply to meet critical loads from both the main power supply and renewable energy sources. Our approach involves processing the network switch information for identifying the number of isolated paths N_{IP}, isolated combinations N_{IC}, and connected combinations N_{CC} in the network. The total number of possible paths/combinations available to supply critical loads is represented as N_{PC} ($N_{PC} = N_{IP} + N_{IC} + N_{CC}$). An isolated path N_{IP} represents a scenario where a single critical load is supplied by only one available source, as shown in Fig. 4. In this case, only the critical load at node 48 is supplied by the source at node 49, and the critical load at node 76 is not supplied by any sources as there is no path available due to the switch status. For a given switch configuration, there can be multiple isolated paths, each supplying a single critical load with more than one available source through individual isolated paths. An isolated combination N_{IC} involves combinations of isolated paths where two or more available sources supply all available critical loads, as shown in Fig. 5, but these paths have no interconnections. Alternatively, a connected combination N_{CC} denotes combinations of paths where two or more available sources supply all available critical loads, as shown in Fig. 6, but these paths are interconnected. Thus, the choice of assigning weights to these three categories is based on the criteria that the highest preference is to be given for the connected combinations, the second highest for isolated combinations, and the least preference for the isolated paths. In our analysis, we have considered the following weights [0.1, 0.4, 0.5] for each category, respectively. Isolated paths, assigned a minimal weight of 0.1, are perceived as the least favorable in terms of resilience. These paths represent singular and direct routes to critical loads without any backup, making their resilience contribution minimal. Conversely, isolated combinations are weighted substantially more at 0.4, as they offer a more robust resilience aspect. Although they consist of multiple supply paths to all necessary critical loads, the lack of interconnections among these paths reduces their flexibility in providing supply from two or more sources. The most valued configuration within this framework is the connected combinations which carry the highest weight of 0.5. It is to be noted that different weights could be given for each category, but the order of preference should remain the same. This preference is attributed to their structure, which facilitates

interconnections among various supply paths, significantly enhancing the network's capability to adapt to and recover from adverse events.

The path variability is determined by multiplying these weights by the actual values of isolated paths, isolated combinations, and connected combinations, as shown below,

$$PV_{CL} = 0.1 \cdot N_{IP} + 0.4 \cdot N_{IC} + 0.5 \cdot N_{CC} \tag{1}$$

3.2.2. Ratio of critical loads served

Understanding the critical loads served helps in assessing the resilience of the power distribution infrastructure to meet the needs of essential loads and services, thereby contributing to the overall resilience and dependability of the power system. The ratio of critical loads served (N_{CLS}) is defined as the ratio of the power supplied to critical loads to the total power demand of critical loads. Mathematically, it is expressed as:

$$N_{CLS} = \frac{P_{CL}}{P_{TCL}} \tag{2}$$

where, P_{CL} is the power supplied to critical loads and P_{TCL} is the total power demand of critical loads. This formula calculates the proportion of power dedicated to critical loads relative to the overall power demand of critical loads. This represents the system's ability to meet the needs of critical loads during normal or disrupted conditions.

3.2.3. Average rating of service

Another parameter for evaluating the resilience of power distribution networks is the average rating of service (A_{RoS}). This parameter emphasizes the accessibility of critical load supplies from both primary and renewable energy sources and assesses the system's capability to handle additional loads beyond its critical load demand. This parameter is also not available in the literature and is proposed considering the IEEE definition of resilience, with the primary goal of providing supply to critical loads. A higher value resulting from this evaluation signifies an additional capacity to fulfill extra load demand. In other words, the system not only meets its essential operational requirements but also has the surplus capacity to accommodate additional loads, ensuring flexibility in its performance. The rating of service (RoS) is computed as the cumulative sum for each isolated path, isolated combination, and connected combination in the network as follows:

$$RoS = \sum_{i=1}^{N_{PC}} \left[\frac{R_{Source} - R_{CL}}{R_{Source}} \right]_i \tag{3}$$

where, R_{Source} is the rating of available sources in kVA and R_{CL} is the rating of critical loads in kVA. N_{PC} is the total number of possible paths and combinations available to supply critical loads. Then, the average for the RoS is computed in the network as follows,

$$A_{RoS} = \frac{N_{CL}}{N_{TCL}} \times \frac{RoS}{N_{PC}} \tag{4}$$

where N_{CL} is the number of critical loads supplied and N_{TCL} is the total number of available critical loads.

3.3. Parameters for topological characteristics

For a given EDS, a topological complex network G is created considering nodes N as substations, buses, or key components of the system and edges E as the physical or electrical connections between them as shown in Fig. 7.

3.3.1. Percolation threshold for topological network

The percolation threshold is a critical probability point in percolation theory that marks the transition between two distinct phases of connectivity in a system [47]. This threshold is not merely a theoretical construct but has practical implications across various domains, from understanding fluid flow in porous materials [48] to the spread of diseases [49] and the robustness of complex networks [50].

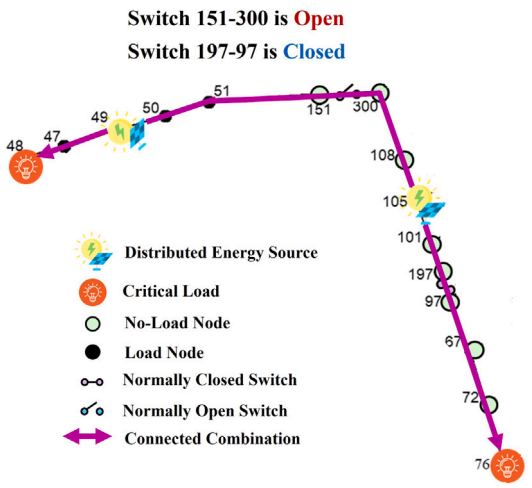

Fig. 6. Connected combination of two sources and two critical loads.

Percolation theory encompasses several models, with site percolation and bond percolation being the most prominent. In site percolation, individual nodes on a network are randomly assigned with a probability p, and the system transitions from isolated nodes to large connected clusters as p increases. The percolation threshold, p_m marks the critical probability at which an infinite, spanning cluster forms. Bond percolation follows a similar logic, with the links or edges between nodes becoming randomly occupied. The threshold p_m again signifies the emergence of a spanning cluster but through the connections between nodes.

When the percolation threshold is high, the system demonstrates an ability to withstand multiple faults or disruptions without significant loss of overall connectivity, as shown in Fig. 8. Alternatively, a low percolation threshold signifies a fragile system that is prone to losing connectivity with just a few failures, highlighting a more isolated network. Thus, the percolation threshold provides crucial insights into the EDS's ability to maintain connectivity and effectively assess resilience against potential disruptions [51].

To evaluate the resilience of a network, we calculate the percolation threshold by evaluating the network's ability to maintain connectivity and deliver power under challenging conditions. The percolation strength is defined as,

$$P_\infty(p) = \frac{1}{NT} \sum_{i=1}^{T} S_i(p) \tag{5}$$

where N is the number of nodes in the network, T is the total number of independent i realizations of the Monte Carlo simulation, $S_i(p)$ is the size of the largest cluster in the network during the ith realization when the bond occupation probability is p which is defined as $\frac{e}{E}$, where e is the number of edges added and E is the total number of edges in the network.

Thus, percolation strength calculates the average size of the largest cluster, normalized by the number of nodes N, averaged over a total number of T independent realizations. This gives a measure of the percolation strength at a given bond occupation probability p. The susceptibility is defined as,

$$\chi(p) = \frac{\left(\frac{1}{N^2 T} \sum_{i=1}^{T} S_i(p)^2\right) - \left[P_\infty(p)\right]^2}{P_\infty(p)} \tag{6}$$

The susceptibility measures the fluctuations in the size of the largest cluster. The numerator consists of two parts: $\frac{1}{N^2 T} \sum_{i=1}^{T} S_i(p)^2$ represents the average of the squares of the sizes of the largest clusters, normalized by N^2. Squaring $S_i(p)$ emphasizes larger clusters more

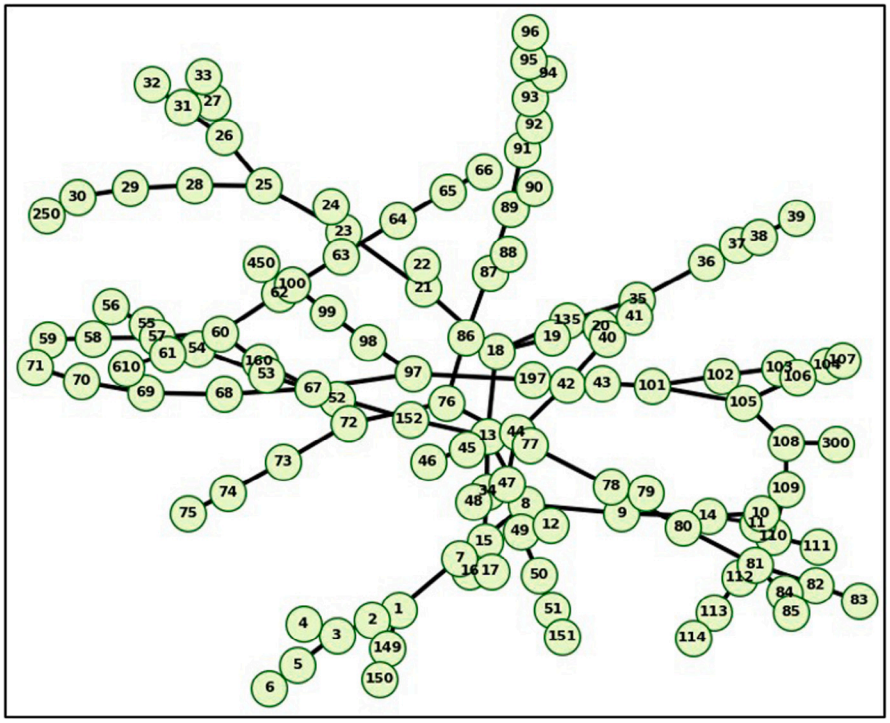

Fig. 7. Topological network of IEEE 123 node test feeder given in Fig. 3.

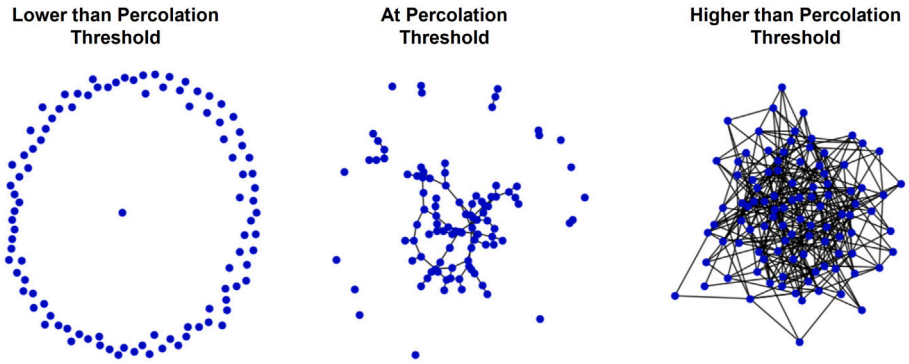

Fig. 8. Stages of network connectivity relative to the percolation threshold: below the threshold, the network remains largely isolated with sparse connections. At the threshold, sufficient connectivity emerges with most nodes. Above the threshold, the network achieves high connectivity, ensuring robust and extensive links throughout.

heavily. $\left[P_\infty(p)\right]^2$ is the square of the average percolation strength, representing the mean of the distribution squared. By subtracting $\left[P_\infty(p)\right]^2$ from $\frac{1}{N^2T}\sum_{t=1}^{T} S_i(p)^2$, we calculate the variance of the size of the largest cluster $S_i(p)$. This variance is a measure of how much the size of the largest cluster fluctuates across different realizations. Normalizing by $P_\infty(p)$ in the denominator makes the susceptibility a relative measure of these fluctuations. The percolation threshold is defined as,

$$p_m = \arg\max_p \chi(p) \tag{7}$$

This identifies the percolation threshold p_m as the value of p that maximizes the susceptibility $\chi(p)$, as shown in Fig. 9. At this critical point, the network undergoes a significant transition from a state of isolated clusters to a state where a giant connected component spans a significant portion of the network. The susceptibility reaches its maximum at p_m, indicating the highest level of fluctuation in the size of the largest cluster.

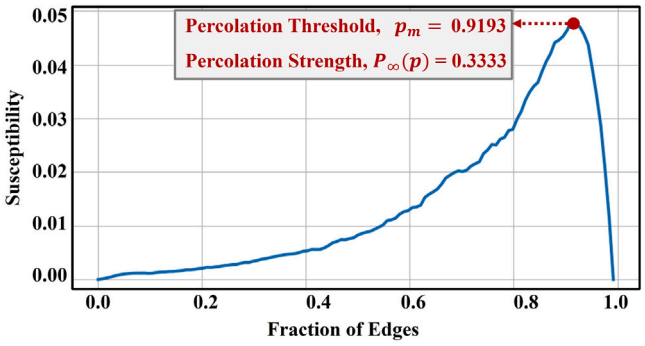

Fig. 9. Susceptibility plot.

Thus, firstly the average size of the largest cluster normalized by the number of nodes is calculated and used to calculate the susceptibility, reflecting the variability in the size of the largest cluster. Lastly, the percolation threshold is determined as the critical point where the network undergoes a significant connectivity transition. This helps in understanding the connectivity properties of a network as edges are added and in identifying the critical point where a giant connected component emerges.

In the context of an electrical network, a higher value of the percolation threshold is anticipated, indicating a network with higher resilience [52]. The process for computation of percolation threshold is explained in Algorithm 1.

Algorithm 1 Compute Percolation Threshold in a Network.

Start
Create: an empty graph G_0 with N nodes and zero number of edges for the considered electrical distribution system.
Initialize: bond occupation probability $p = 0$. Prepare arrays for $P_\infty(p)$ and $\chi(p)$.
for *each realization* i **from** 1 **to** T **do**
  for *each probability* p **increment from** 0 **to** 1 **do**
    Add edges in G_0 according to p.
    Calculate the size of the largest cluster $S_i(p)$.
    Update $P_\infty(p)$ and $\chi(p)$ for the current value of p.
  end for
  Reset $p = 0$.
end for
Compute: the average of $P_\infty(p)$ and $\chi(p)$ over all T realizations.
Find p_m: where $\chi(p)$ reaches the maximum for the value of p.
Return p_m
Stop

3.3.2. Information centrality for system's nodes

The concept of information centrality within a graph provides a valuable means of identifying nodes crucial for maintaining the functionality of a system [53]. The identification of such nodes ensures a reliable and continuous supply of electricity to critical loads. For a graph G with N nodes, the efficiency $E_n[G]$ is calculated using the formula:

$$E_n[G] = \frac{1}{N \cdot (N-1)} \sum_{i=1}^{N} \sum_{j \neq i} \frac{1}{d_{ij}} \tag{8}$$

where d_{ij} represents the shortest path distance between node i and node j. The information centrality, denoted as C_m is computed as follows:

$$C_m = \frac{E_n[G] - E_n[G_0]}{E_n[G]} \tag{9}$$

where $E_n[G]$ represents the network's overall efficiency, reflecting its resilience, and $E_n[G_0]$ is network efficiency after the removal of m node. This physical simulation helps identify nodes whose removal has a significant impact on the network's ability to maintain functionality during disruptions or failures.

The step-by-step approach for computing and ranking information centrality of nodes in the system:

(a) Determine the network's overall efficiency, denoted as $E_n[G]$.
(b) Select node for removal and compute the network's efficiency, $E_n[G_0]$.
(c) Calculate the drop in network efficiency using (9).
(d) Repeat this process for all nodes.
(e) Sort the obtained information centrality of all the nodes. Apply a threshold equal to 0.1 and obtain the number of nodes with higher information centrality N_{HC}. The threshold of 0.1 indicates that nodes considered as central nodes affect the system's efficiency by more than 10% when removed. For the topological network in Fig. 7, the obtained N_{HC} is 16, as shown in Fig. 10, and the obtained values are given in Table 3. It is observed that for the IEEE 123 node test feeder, 16 nodes are considered central nodes. Only 2 of these nodes affect the system's efficiency by more than 20%, while the rest affect the system's efficiency between 10% and 20%. Thus, increasing the threshold beyond 20% would result in an insufficient number of central nodes for an effective resilience evaluation of the EDS.

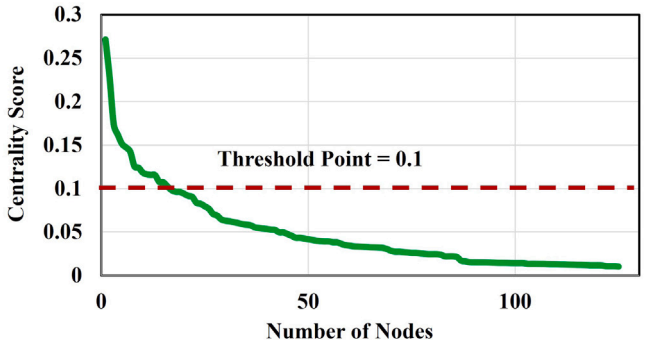

Fig. 10. Centrality scores computation for all 123 nodes in the network given in Fig. 7. The threshold point equal to 0.1 is considered for the analysis. In total, we got 16 nodes having information centrality scores above the threshold, tabulated in Table 3 and thus, N_{IC} for the network is 16.

Table 3
16 Nodes with centrality score above threshold for the network given in Fig. 7.

Node	Information centrality
13	0.271
18	0.227
8	0.173
67	0.161
54	0.151
21	0.147
60	0.142
23	0.125
97	0.124
152	0.118
53	0.116
52	0.115
76	0.115
25	0.107
35	0.107
7	0.102

3.4. Proposed resilience metric

The evaluation of power distribution infrastructure resilience adopts a comprehensive approach that considers both functional dynamics and topological characteristics within the network. The weighted analysis of path variability takes into consideration the availability of critical load supplies, offering a functional perspective on resilience. The parameters associated with the ratio of critical loads served and the average rating of service provide valuable insights into the system's capacity to meet power demands and ensure the continued availability of critical services. Additionally, utilizing percolation threshold analysis allows for a deeper understanding of the network transitions from efficient operation to a state susceptible to cascading failures. The identification of information centrality focuses on key nodes essential for sustaining network efficiency. This multi-faceted approach not only enhances the assessment of resilience but also provides actionable information for strategic improvements in the power distribution infrastructure.

Table 4
Pairwise comparison matrix with weight coefficients for each parameter.

Parameter	PV_{CL}	N_{CLS}	A_{RoS}	p_m	N_{HC}	W
PV_{CL}	1	2.5	10	2.5	10	**0.50**
N_{CLS}	0.4	1	4	1	4	**0.20**
A_{RoS}	0.1	0.25	1	0.25	1	**0.05**
p_m	0.4	1	4	1	4	**0.20**
N_{HC}	0.1	0.25	1	0.25	1	**0.05**

Following the computation of the aforementioned parameters, the resilience metric ($\mathfrak{R}$) is determined as,

$$\mathfrak{R} = R \cdot W^T \tag{10}$$

where,

$$R = [PV_{CL}, N_{CLS}, A_{RoS}, p_m, N_{HC}] \tag{11}$$

$$W = [w_{PV_{CL}}, w_{N_{CLS}}, w_{A_{RoS}}, w_{p_m}, w_{N_{HC}}] \tag{12}$$

The min–max normalization technique is used to normalize each of the five parameters in the proposed resilience metric R. This approach scales all parameters to a uniform range between 0 and 1. After normalization, each parameter is multiplied to their respective weights, denoted by $w_{PV_{CL}}$, $w_{N_{CLS}}$, $w_{A_{RoS}}$, w_{p_m} and $w_{N_{HC}}$ corresponding to the path variability, ratio of critical loads served, and average rating of service, percolation threshold, and number of nodes with higher information centrality, respectively. The analytic hierarchy process (AHP) is utilized to compute the weights of all parameters W [21], which incorporates a structured technique for analyzing complex decisions in the following steps:

1. Define the resilience assessment problem and identify the criteria and alternatives based on system performance.
2. Structure the decision-making hierarchy starting from the overall objective of resilience assessment through various parameters.
3. Construct a set of pairwise comparison matrices R where each criterion is compared against others in terms of its contribution to the system's resilience.
4. Determine the weights of each criterion W using the pairwise comparison matrices. The principal eigenvector of matrix R indicates the relative importance of each criterion.
5. Validate the consistency of the pairwise comparisons by computing the consistency index and the consistency ratio. Ensure that the comparisons are sufficiently coherent to proceed with the analysis.
6. Synthesize the relative weights required to calculate the overall resilience metric $\mathfrak{R}$.

The pairwise comparison matrix for the parameters and their respective weights are given in Table 4. The $w_{N_{CLS}}$ set at 0.20 ensures that essential services remain operational during disruptions, which highlights the system's priority for maintaining crucial operations. The $w_{PV_{CL}}$ valued at 0.50, which has the highest weightage, emphasizes the system's flexibility by offering more alternative routes for power delivery. The $w_{A_{RoS}}$ is set at 0.05 and is of lower priority, as it only assesses the system's capacity to handle additional loads beyond critical needs. The remaining 25% of the weightage is given to the topological parameters, where w_{p_m} set at 0.20 shows the system's resilience by indicating the critical point leading to network fragmentation and where $w_{N_{HC}}$ at 0.05 measures the important nodes within the network impacting the system's resilience.

Further, the composite resilience score for n switch configurations is determined using the following equation [1,21],

$$\mathfrak{R}_C = \mathfrak{R}^{max} + (1 - \mathfrak{R}^{max}) \sum_{a}^{n-1} w_a \mathfrak{R}_a \tag{13}$$

where, $\mathfrak{R}^{max}$ corresponds to the network configuration with the highest resilience score, $\mathfrak{R}_a$ represents the resilience score of the ath switch configuration, and w_a is the respective weight assigned to each ath configuration. The $(1 - \mathfrak{R}^{\max})$ factor ensures that the contribution of the other configurations is scaled appropriately based on the highest resilience score. If the highest resilience score is close to 1, the contribution of other configurations will be smaller. $\sum_{a=1}^{n-1} w_a \mathfrak{R}_a$ is the weighted sum of the resilience scores of the other configurations. The weights w_a should sum to 1 for the weighted average to be meaningful. In this work, we have assigned equal weightage to each switch configuration. A detailed illustration of the proposed methodology for resilience evaluation in EDS is shown in Fig. 11.

Each switch configuration of the EDS must adhere to operational constraints, including power balance, node voltage limits, and feeder current capabilities. The constraints on node voltage levels and branch capacities are given as follows:

Voltage limits constraint:

$$|V_n^{min}| \le |V_n| \le |V_n^{max}| \tag{14}$$

Branch current capability constraint:

$$|I_{f,n}| \le |I_{f,n}^{max}| \tag{15}$$

$$|I_{b,n}| \le |I_{b,n}^{max}| \tag{16}$$

Output power constraints distributed generation:

$$P_{\mathrm{DG}}^{min} \le P_{\mathrm{DG}} \le P_{\mathrm{DG}}^{max} \tag{17}$$

$$Q_{\mathrm{DG}}^{min} \le Q_{\mathrm{DG}} \le Q_{\mathrm{DG}}^{max} \tag{18}$$

In the equations above, V_n denotes the voltage at node n, $I_{f,n}$ represents the forward branch current for the nth distribution line, and $I_{b,n}$ signifies the reverse branch current for the nth distribution line. P_{DG} and Q_{DG} are the real and reactive power outputs from distributed generators, respectively. The subscripts *min* and *max* indicate the minimum and maximum permissible limits for the respective parameters. In this work, we consider a constraint on the voltage that the variations must not exceed a ± 0.05 p.u. [1]. For each switch configuration, the power flow constraints and voltage limits are verified to ensure they are within permissible limits. Then the resilience metric $\mathfrak{R}$ is determined for each switch configuration using Eq. (10).

4. Proposed methodology for resilience evaluation

In the standard IEEE 123 node test feeder, there are 12 switches, out of which 6 are normally closed and 6 are normally open. Table 5 outlines the considered cases for resilience evaluation, focusing on the operation of normally closed and normally opened switches shown in Fig. 3. In Case A, we operate normally closed switches. In Cases B and C, two normally open switches, 151–300 and 54–94, were operated, respectively. Subsequently, in Case D, both normally open switches were operated with the standard operation of a closed switch. For each case, we have specified configurations based on the status of closed switches, Sw1, Sw2, Sw3, and Sw4, shown in Table 6. Further, for the enhancement of resilience, two additional switches, 36–57 and 55–81, are added to the network for Case A to D and are referred to as Case A_add, Case B_add, Case C_add, and Case D_add, respectively. The positions for new switches were selected in accordance with optimal switch allocation principles given in [54].

For each switch configuration, a complex topological network is created as shown in Fig. 7, and then computed topological parameters for resilience metrics, i.e., percolation threshold and number of central nodes in the network. Then, using the information on the network configuration, critical loads, and available power supply, all the possible paths/combinations for serving critical loads are identified, and the power flow and voltage constraints are checked. All three electrical

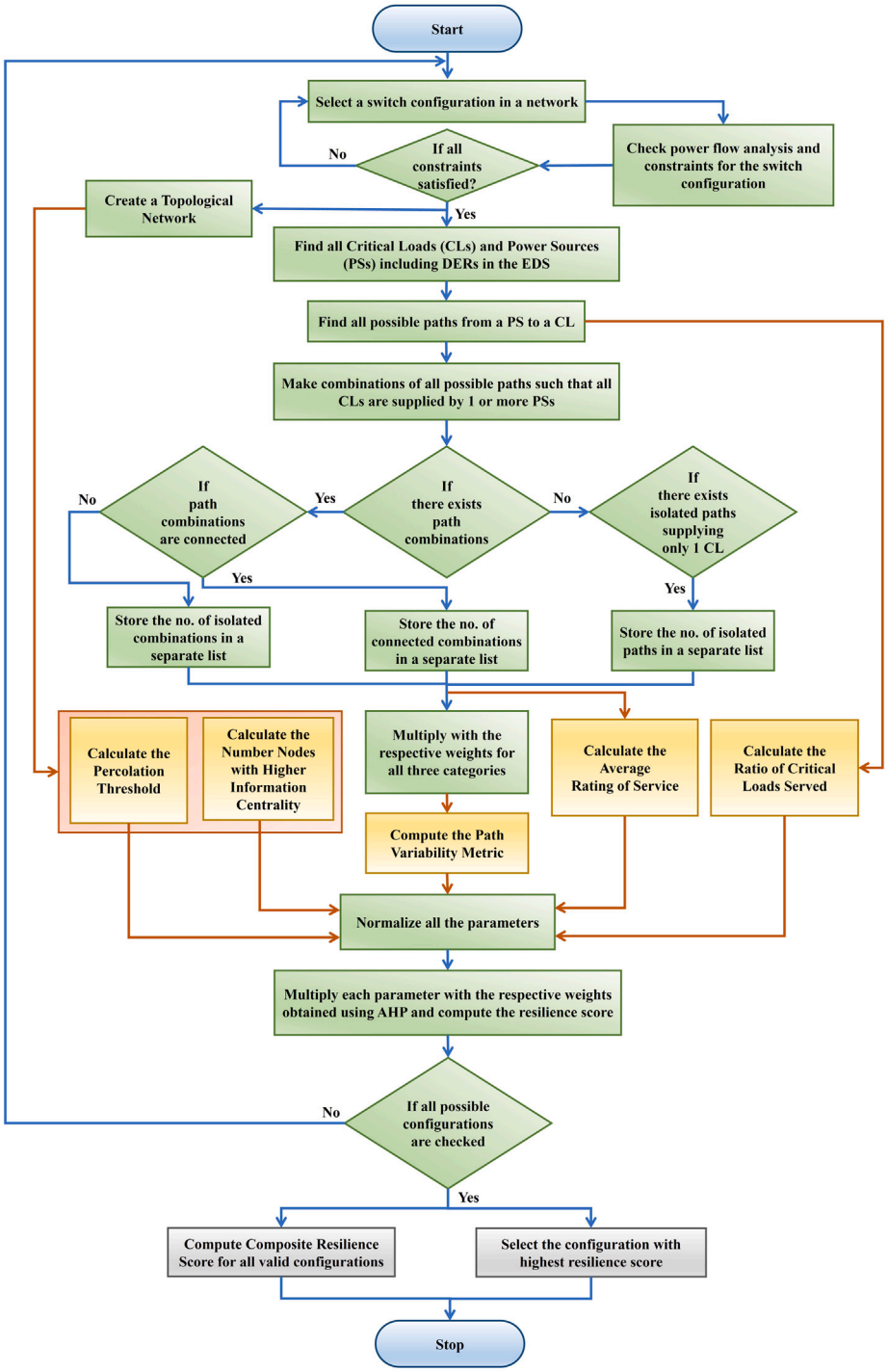

Fig. 11. Methodology for evaluating electrical distribution system resilience using the proposed comprehensive metric.

service parameters are computed, i.e., weighted path variability, ratio of critical loads served, and average rating of service. Using AHP, computation of weights is achieved as shown in Table 4. Finally, all five parameters are multiplied by their respective weights, which provides the resilience score $\Re$. The detailed explanation for the proposed methodology is illustrated in Fig. 11. This proposed methodology is suitable for computing resilience for planning as well as operations of EDS. It helps in evaluating the system's resilience during extreme events and also identifies the switching topology that could help restore the system's operation back to normal. Also, it allows the evaluation of the system's resilience while planning resilience enhancement techniques.

5. Simulation results and discussion

Using the proposed methodology, the resilience is evaluated for the EDS under various conditions, such as existing switch configurations, additional switches, and DER integration.

5.1. Resilience evaluation for existing network

Considering the operation of the 4 normally closed switches (Case A) in the IEEE 123 node test feeder, there are 16 switch configurations, as shown in Table 6. Then, using paths/combinations information

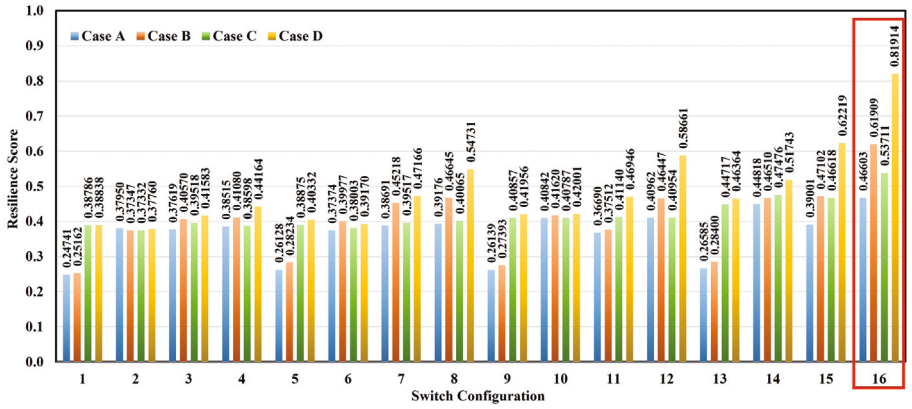

Fig. 12. Resilience scores obtained for considered cases based on switches operations of all subcases.

Table 5
Considered cases for resilience evaluation based on switches.

Cases	Switches operation
Case A	Standard operation of closed switches.
Case B	Operation of switch 151-300 and standard operation of closed switches.
Case C	Operation of switch 54-94 and standard operation of closed switches.
Case D	Operation of both switches 151-300 and 54-94 and standard operation of closed switches.

Two additional switches, 36-57 and 55-81, are operated with the above cases and are referred to as Case A_add, Case B_add, Case C_add, and Case D_add, respectively.

Table 6
Switch configuration.

Subcase	Sw1 13 to 152	Sw2 18 to 135	Sw3 97 to 197	Sw4 60 to 160
1	0	0	0	0
2	0	0	0	1
3	0	0	1	0
4	0	0	1	1
5	0	1	0	0
6	0	1	0	1
7	0	1	1	0
8	0	1	1	1
9	1	0	0	0
10	1	0	0	1
11	1	0	1	0
12	1	0	1	1
13	1	1	0	0
14	1	1	0	1
15	1	1	1	0
16	1	1	1	1

Sw5 (150 to 149) and Sw6 (61 to 610) are closed for all cases.

mentioned in Table 7 for all 16 configurations, the parameter PV_{CL} is computed. All computed parameters of the proposed resilience metric for Case A are tabulated in Table 8. It is observed that configuration 16 has the highest resilience score of 0.466, achieved when all four switches are closed.

Further, we calculated resilience scores for all 16 configurations for the considered four cases mentioned in Table 5. The results are analyzed to evaluate the resilience scores under normal operating conditions. The obtained results are shown in Fig. 12; it is observed that the resilience score for Case D is significantly higher. The configuration 16 of Case D achieves the highest resilience score of 0.81914; this shows the potential to enhance system resilience by strategically utilizing the available normally closed and open switches within the system.

Table 7
Number of paths and combinations obtained for Case A.

Case A	N_{IP}	N_{IC}	N_{CC}	PV_{CL}
1	1	0	0	0.1
2	0	1	0	0.4
3	0	1	0	0.4
4	0	2	0	0.8
5	3	0	0	0.3
6	0	3	0	1.2
7	0	3	0	1.2
8	0	6	0	2.4
9	1	0	0	0.1
10	0	3	0	1.2
11	0	1	0	0.4
12	0	4	0	1.6
13	4	0	0	0.4
14	0	6	10	7.4
15	0	4	0	1.6
16	0	10	15	11.5

5.2. Resilience enhancement with additional switches

Enhancing the resilience of the EDS is effectively achieved through the strategic placement of additional switches. Moreover, the integration of smart switches equipped with remote control and automation capabilities enables swift responses to issues, improving the system's adaptability and efficiency. Two additional switches, 36–57 and 55–81 are integrated into the system [1]. Case D with these additional switches is considered, and resilience scores are obtained as shown in Fig. 13. The results are compared for Case D and Case D_add; it is observed that the system's resilience could be improved to 0.87554 with the integration of additional switches.

5.3. Resilience enhancement with integration of DERs

The integration of DERs is a key strategy for enhancing the resilience of EDS. DERs, such as solar panels, wind turbines, energy storage systems, and other distributed generation sources, contribute to a more robust and flexible energy infrastructure. DERs provide a decentralized source of power, reducing dependency on centralized generation. This decentralization inherently improves the system's ability to withstand and recover from disruptions, such as natural disasters or equipment failures. In the event of a grid outage, DERs could operate autonomously, supplying power to critical loads and essential services.

The DERs are introduced into the system at different nodes. At first, a single DER is integrated at Node 49, denoted as 1 DER. Following this, two DERs are added at Nodes 49 and 56, labeled as 2 DER. The

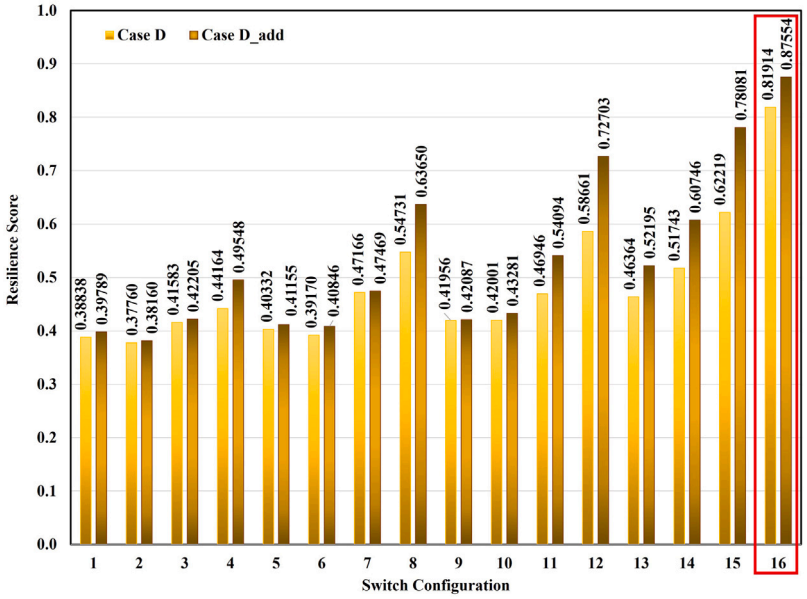

Fig. 13. Resilience scores obtained with the placement of additional switches for Case D. The resilience is improved in comparison to the system operating with existing switches.

Table 8
Resilience scores for Case A.

Case A	N_{HC}	p_m	PV_{CL}	N_{CLS}	A_{RoS}	$\mathfrak{R}$
1	9	0.758	0.100	0.460	0.058	0.247
2	13	0.835	0.400	1.000	0.198	0.379
3	13	0.818	0.400	1.000	0.198	0.376
4	15	0.852	0.800	1.000	0.198	0.385
5	15	0.793	0.300	0.460	0.169	0.261
6	16	0.730	1.200	1.000	0.421	0.374
7	17	0.795	1.200	1.000	0.421	0.387
8	20	0.789	2.400	1.000	0.421	0.392
9	16	0.826	0.100	0.460	0.058	0.261
10	21	0.902	1.200	1.000	0.421	0.408
11	18	0.770	0.400	1.000	0.198	0.367
12	25	0.911	1.600	1.000	0.365	0.410
13	19	0.820	0.400	0.460	0.141	0.266
14	24	0.927	7.400	1.000	0.494	0.448
15	23	0.813	1.600	1.000	0.365	0.390
16	27	0.927	11.500	1.000	0.441	0.466

analysis extends further by incorporating three DERs at Nodes 49, 56, and 105, referred to as 3 DER. Lastly, a configuration involving four DERs at Nodes 49, 56, 105, and 21 is examined and labeled as 4 DER. This systematic progression allows us to assess the resilience of the system under various DER integration scenarios, starting from the base case, i.e., no DERs, and gradually introducing additional DERs at specific nodes. With various levels of DER integration, resilience scores are obtained for Case D as shown in Fig. 14. It is observed that with the integration of DERs, system resilience has been improved. In configuration 16 of Case D, the resilience score shows significant enhancement, increasing from 0.44353 for the base case to 0.81914 for 4 DERs. The composite resilience of each considered case with variation in DERs integration has been shown in Table 9. Thus, it has been observed that the proposed metric has the capability to evaluate the system's resilience during planning.

As some of the considered cases in this work are similar to those in M6 [1], a quantitative comparison is provided in Table 10. The topological resiliency index (TRI) and feasible network resiliency index (FNRI) scores computed in M6 are compared with the proposed resilience metric scores for similar scenarios involving DER integration and additional switches. As discussed in Section 1, these quantitative comparisons offer a limited understanding of the resilience evaluation

Table 9
Composite resilience scores for different cases.

Case	No. of DERs	$\mathfrak{R}_a$
Case A	No DER	0.56623
Case A	1 DER	0.59270
Case A	2 DERs	0.60810
Case A	3 DERs	0.61603
Case A	4 DERs	0.64465
Case B	4 DERs	0.75651
Case C	4 DERs	0.71452
Case D	4 DERs	0.89754
Case D_add	4 DERs	0.93512

Table 10
Comparison of resilience scores with M6.

Cases	TRI scores	FNRI scores	Proposed metric scores
Base Case	0.5977	0.2652	0.5662
2 DERs	0.6516	0.6614	0.6081
3 DERs	–	0.7519	0.6160
4 DERs	0.7626	0.8875	0.6446
Base case + additional switches	0.9312	0.4022	–
2 DERs + additional switches	0.9314	0.8808	–
3 DERs + additional switches	–	0.9254	–
4 DERs + additional switches	–	0.9329	–
4 DERs + open switches	–	–	0.8975
4 DERs + open & additional switches	–	–	0.9351

criteria and considerations. These comparisons primarily illustrate the relative changes in resilience scores across different scenarios.

6. Case studies with various extreme events

By using the proposed metric, power system engineers could proactively engage in long-term strategic planning before encountering any contingencies. In this section, the effectiveness of the proposed algorithm is demonstrated by providing key factors in decision-making for operational resilience. The resiliency scores under different operating conditions assist the power distribution system's operator in making decisions in order to meet critical load requirements under varied contingency scenarios.

We consider contingency events such as floods, wildfires, hurricanes, and short-circuit faults. Each of these events causes damage to

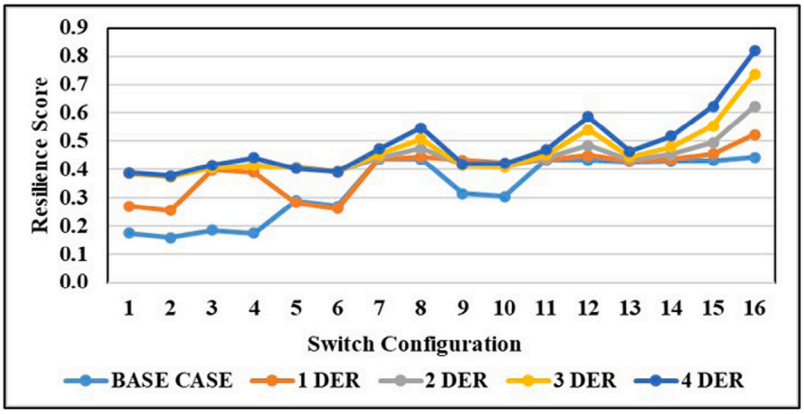

Fig. 14. Resilience scores with DERs integration in the system for Case D.

the infrastructure of the distribution system and affects the electric service to the critical loads. The extent of the damage caused by each event is listed in Table 11. In this study, the considered events are presented as illustrative examples based on their typical characteristics and patterns. The correlation between event types and affected system components in Table 11 follows typical damage patterns: hurricanes cause the most extensive damage (affecting 41 nodes and 50 lines), floods impact moderate areas (affecting 25 nodes and 28 lines), and wildfires cause relatively concentrated damage (affecting 22 nodes and 25 lines), while short-circuit faults typically result in localized impacts (affecting 2 transmission lines). While detailed weather event modeling using historical data could enhance event prediction accuracy, and impact assessment methods like fragility curves could improve damage estimation; the proposed metric focuses on resilience evaluation once component failures are identified. The actual extent and severity of damage in real-world scenarios would vary depending on the event intensity, geographical location, and other factors specific to each event. The development of detailed weather modeling and impact assessment methods integrated with the proposed resilience metric could be considered in future works. For all contingency analyses, we assume that damaged nodes and lines are automatically isolated through protective devices at the buses. While these protection devices are not shown in Fig. 3, their operation is critical for isolating affected sections and enabling the evaluation of remaining paths to serve critical loads through various switching configurations.

Table 11
List of damaged components for each contingency event.

Event	Load nodes	No-Load Nodes	Switches	Power Sources	No. of lines
I	1, 2, 4, 5, 6, 7, 9, 10, 11, 12, 16, 17, 19, 20, 22, 24. **(16 nodes)**	149, 3, 8, 13, 14, 15, 18, 23, 135. **(9 nodes)**	150–149, 13–152, 18–135. **(3 switches)**	Main Supply, DER at node 21 **(2 sources)**	**28**
II	73, 68, 69, 70, 71, 98, 99, 100, 102, 103, 104. **(11 nodes)**	60, 61, 610, 160, 67, 72, 97, 197, 101, 450. **(10 nodes)**	61 – 610, 60 – 160, 97 – 197. **(3 switches)**	DER at node 56 **(1 source)**	**25**
III	1, 2, 4, 5, 6, 7, 9, 10, 11, 12, 17, 96, 94, 52, 53, 58, 59, 68, 69, 70, 71, 74, 75, 98, 99, 100. **(26 nodes)**	149, 3, 8, 14, 13, 15, 152, 54, 57, 60, 160, 67, 97, 197, 450. **(15 nodes)**	150 – 149, 13 – 152, 60 – 160, 97 – 197, 36 – 57. **(5 switches)**	Main Supply. **(1 source)**	**50**
IV	–	–	–	–	**2**

6.1. Contingency I: Flood

For operational resilience evaluation, we take flood contingency into account, as shown in Fig. 15. This incident disrupts the power supply from the main substation, prompting the utilization of four available DERs to sustain the supply and fulfill the demand for critical loads [55]. As tabulated in Table 11, a total of 16 load nodes, 9 no-load nodes, 3 switches, 2 power sources, and 28 lines are damaged. Considering the existing network, the topological network parameters and the parameters relevant to supplying critical loads are computed. Subsequently, resilience scores for the 16 switching configurations are computed for Cases A to D, and the highest scores are obtained for Case D and shown in Fig. 16. Out of the 16 switch configurations, only 4 configurations have the ability to meet the critical load demand through paths/combinations. Though the remaining 12 configurations cannot meet the critical load demand, they still have some resilience values, indicating that they still have the infrastructure available to supply critical loads. Configuration 4 has the highest resilience score, 0.4377, and is the preferred switch configuration during this extreme event.

For the same fault condition, a resilience curve is obtained as shown in Fig. 17, which provides insights into how switching operation influences the system's resilience [13]. The resilience curve is constructed using the proposed resilience metric. The curve is drawn considering the planning and operational resilience and it visually captures the impact of strategies on the system's ability to withstand and recover from adverse events. Initially, at point A, the system operates with 4 DERs with a resilience score of 0.6447, indicating the normal operation of the system. Following the flood event, the system transitions into a degraded state at point C, with its resilience reduced to 0.4161, reflecting the immediate impact of the disruption. At point D, the resilience score is 0.5494; the system shows initial recovery efforts using the switching action of existing switches in the network under fault conditions. After the infrastructure is restored to its initial state, the system's resilience score returns to its original value of 0.6447 at points E and F, indicating full recovery from the immediate impacts

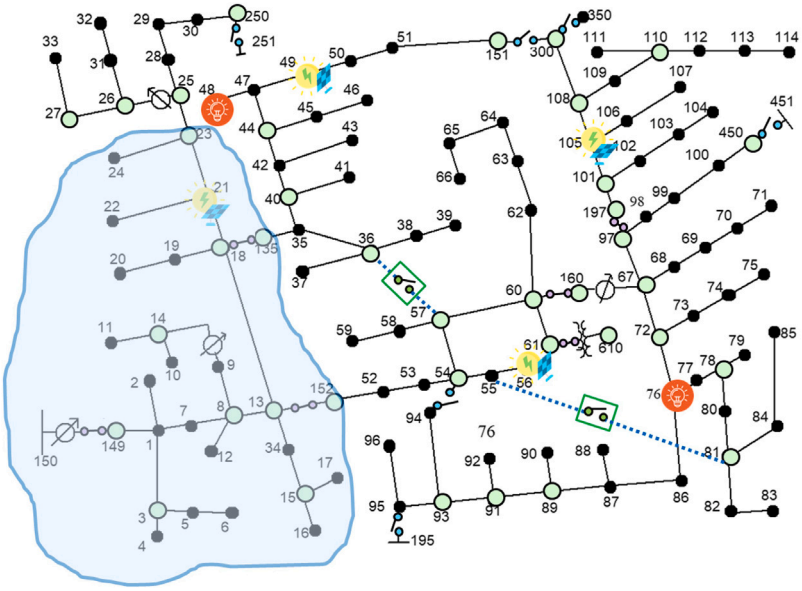

Fig. 15. Contingency I: Flood.

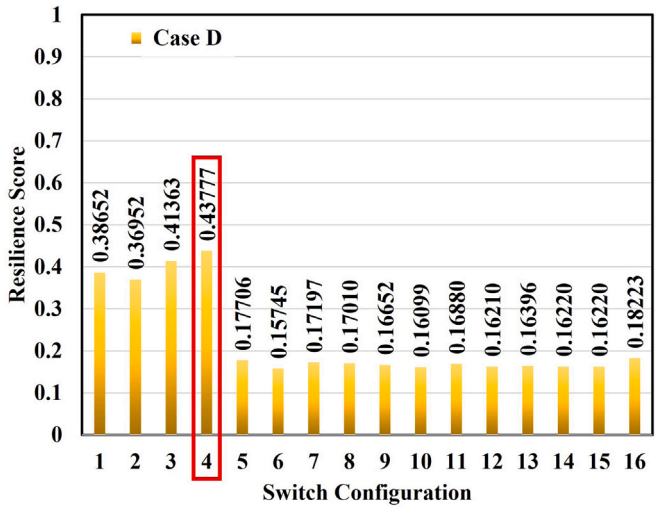

Fig. 16. Resilience scores for possible switches topology during contingency I: Flood.

of the fault event. The return to Case A reflects the system reverting to normal operation, balancing all loads and other operational factors beyond system resilience. Once the system is restored, the system operator could consider enhancing the resilience further by selecting the existing switches in the network to 0.8975 at points G and H. The resilience could be further enhanced at point I with a resilience score of 0.9351 where the system achieves its highest resilience using additional switches. The inclusion of these points highlights the ongoing nature of resilience planning and the potential for continuous improvement. It also acknowledges that while resilience is crucial, DSOs must balance it with other operational factors and constraints in their decision-making process. This approach provides a comprehensive view of both immediate and long-term resilience strategies.

6.2. Contingency II: Wildfire

Disturbances in EDS and the vulnerability of the infrastructure, particularly in conditions of heightened fire risk, could potentially trigger the onset of wildfires [56]. The source of power distribution system faults are diverse, falling into categories such as vegetation-related issues, failures in electrical apparatus, deficiencies in poles and cross-arms, and line failures [57,58]. The wildfire event is considered as shown in Fig. 18. The affected network is isolated, and using available sources, the critical load demands are met. As tabulated in Table 11, a total of 11 load nodes, 10 no-load nodes, 3 switches, 1 power source, and 25 lines are damaged. The possible switch configurations are identified and the resilience scores are computed for Case A to D. The results of Case D are shown in Fig. 19, the configuration 13 has the highest resilience score of 0.43444. Other configurations 1, 5, and 9 are also able to meet the CL demand through possible paths/combinations, while the remaining configurations only have the infrastructure resilience parameters.

The resilience curve for wildfire event is shown in Fig. 20. Initially, the system is operational with 4 DERs with a resilience score of 0.6447. Subsequent to the onset of a wildfire event, the resilience score is reduced to 0.3082 at point C, which quantitatively reflects the acute degradation of system operation. Through the application of strategic grid reconfiguration, the resilience score is improved to 0.5395 at point D, indicating preliminary restoration efforts. Further, the resilience reaches points E and F, where the metric is restored to its initial value of 0.6447, showing full operational recovery from the wildfire's perturbations. Once the system is restored, the system operator could consider enhancing the resilience further by selecting the existing switches in the network to 0.8975 at points G and H. The resilience enhancement phase culminates at the point I, where the system's resilience metric peaks at 0.9351, achieved through the implementation of infrastructural modifications.

6.3. Contingency III: Hurricane

Meteorological records indicate that hurricanes typically form in the ocean and advance toward continents. Upon landfall, the hurricane's intensity swiftly diminishes as it progresses further inland, influenced by the finite heat capacity of the soil surface. Consequently, distributed systems located in coastal areas bear the brunt of the most severe damage during a hurricane event. The system is assumed to have been impacted by a severe hurricane [59], resulting in approximately half of the nodes and connecting lines being impaired as shown in Fig. 21. As tabulated in Table 11, a total of 26 load nodes, 15 no-load nodes, 5 switches, 1 power source, and 50 lines are damaged. This hurricane has led to the formation of two islands, where the supply of critical loads

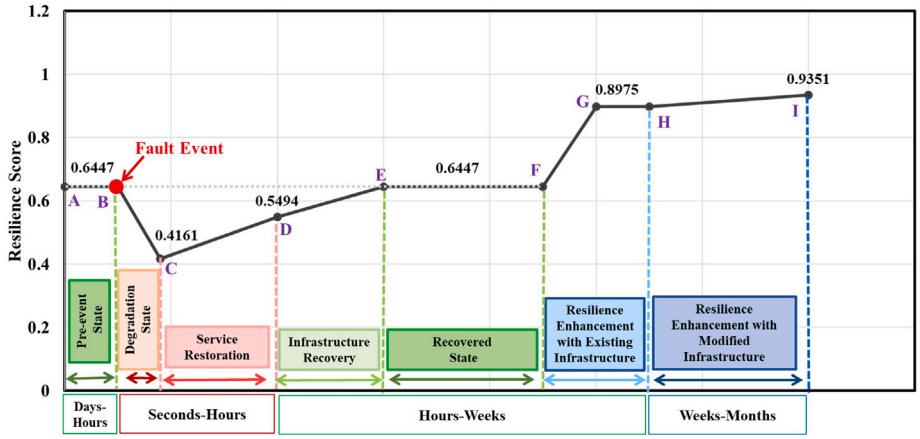

Points	Case Details
A & B	Case A with 4 DERs.
C	Case A with 4 DERs under event conditions.
D	Case D with 4 DERs under event conditions.
E & F	Case A with 4 DERs after recovering from an extreme event.
G & H	Case D with 4 DERs after recovering from an extreme event.
I	Case D with additional switches with 4 DERs after recovering from an extreme event.

Fig. 17. Resilience curve during contingency I: Flood.

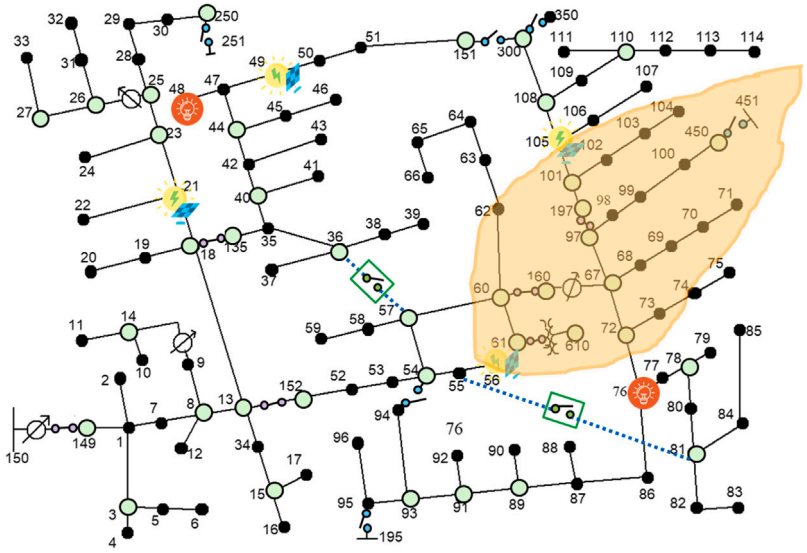

Fig. 18. Contingency II: Wildfire.

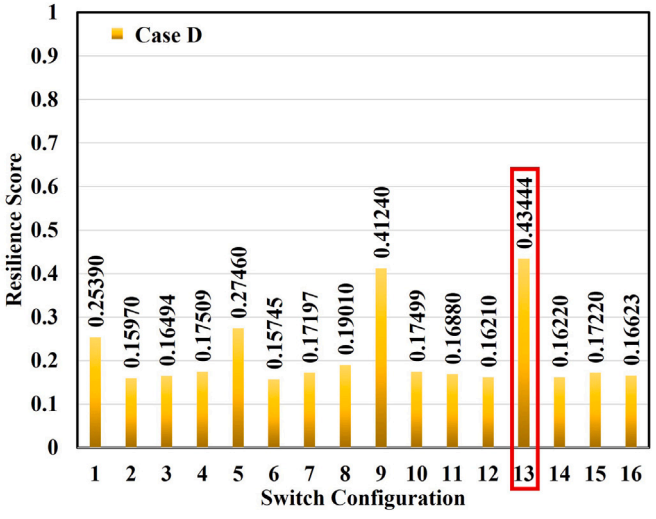

Fig. 19. Resilience scores for possible switches topology during contingency II: Wildfire.

could only be maintained through integrated DERs of the network. There are only two switch configurations where only isolated paths are available for supplying critical loads in Case A and Case B, while Case C and Case D do not have any paths/combinations in all configurations to supply CLs. Case B has the highest resilience score, with configuration 5 having a score of 0.26719, as shown in Fig. 22.

The system initially has a resilience score of 0.6447 at point A, indicating the initial resilience as shown in the resilience curve for Fig. 23. The system is affected by a severe hurricane, leading to a significant drop in resilience to 0.2658 at point C, showcasing the immediate adverse effects on the system's functionality. Switching to Case D is strategic employment by the existing network switches for initial recovery with a resilience score of 0.3492. After some time, restoration continues, and the system's resilience reaches again to 0.6447 at points E and F, showing a complete recovery from the hurricane's impacts. After the restoration of the system, the operator could plan to enhance the resilience further by selecting the existing switches in the network to 0.8975 at points G and H. Through additional infrastructure enhancements and strategic DER integration, the system achieves its highest resilience score of 0.9351, showing at point I. This final state not only signifies a full recovery but also an enhanced preparedness, equipping the system with superior resilience against future disruptions and illustrating a significant advancement from its initial resilience capabilities.

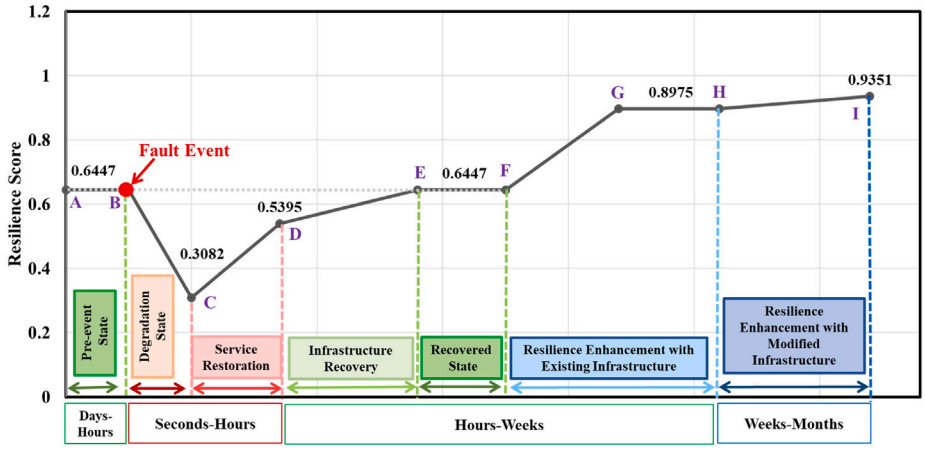

Points	Case Details
A & B	Case A with 4 DERs.
C	Case A with 4 DERs under event conditions.
D	Case D with 4 DERs under event conditions.
E & F	Case A with 4 DERs after recovering from an extreme event.
G & H	Case D with 4 DERs after recovering from an extreme event.
I	Case D with additional switches with 4 DERs after recovering from an extreme event.

Fig. 20. Resilience curve during contingency II: Wildfire.

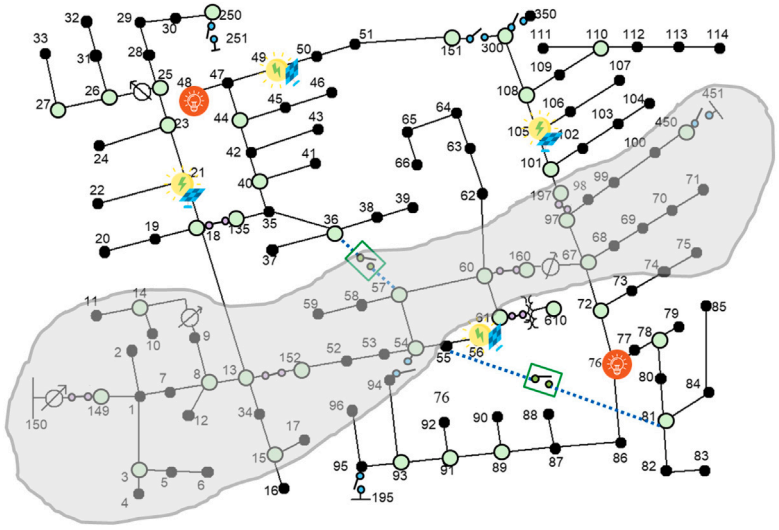

Fig. 21. Contingency III: Hurricane.

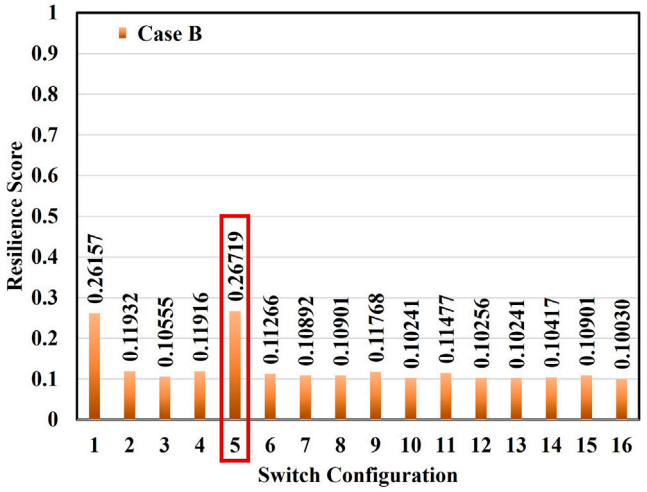

Fig. 22. Resilience scores for possible switches topology during contingency III: Hurricane.

6.4. Contingency IV: Short circuit event

Another situation is considered as mentioned in Table 11, two three-phase lines between 13–18 and 50–51 are intentionally disconnected or tripped as a result of a fault, such as a short circuit shown in Fig. 24. We have evaluated the resilience scores for various switch configurations for Case A to D and the scores of Case D are shown in Fig. 25. All 16 configurations are able to meet the CLs, and configuration 13 has the highest resilience score of 0.41225, which is even higher than configuration 16 due to the higher values obtained through infrastructure resilience parameters.

The resilience curve for short circuit event is shown in Fig. 26. Initially, at point A, the system is operational with 4 DERs showing a resilience score of 0.6447. During a fault event, the system's resilience reduces to 0.6025 at point C, showing the immediate effects of the disruption. Service restoration begins at point D, where the resilience score rises to 0.6269 using existing switches within the network. This trajectory towards full system recovery is further illustrated as the resilience score is fully restored to 0.6447 at points E and F, indicating the system's rebound from the impacts of the fault event. After the restoration of the system, the operator could plan to enhance the resilience further by selecting the existing switches in the network to 0.8975 at points G and H. The resilience enhancement is observed at point I through the application of additional infrastructural modifications and the system reaches a peak resilience score of 0.9351.

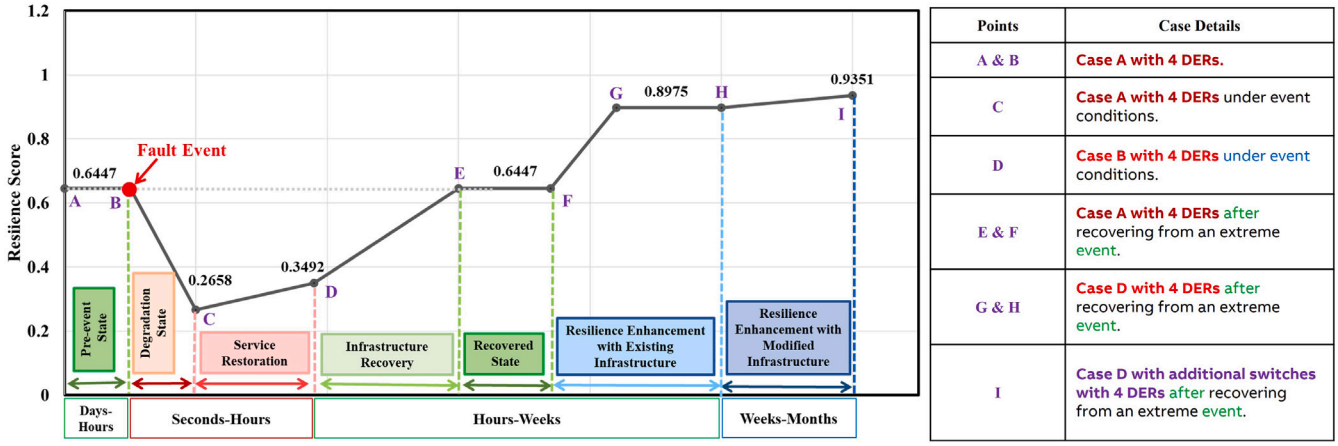

Points	Case Details
A & B	Case A with 4 DERs.
C	Case A with 4 DERs under event conditions.
D	Case B with 4 DERs under event conditions.
E & F	Case A with 4 DERs after recovering from an extreme event.
G & H	Case D with 4 DERs after recovering from an extreme event.
I	Case D with additional switches with 4 DERs after recovering from an extreme event.

Fig. 23. Resilience curve during contingency III: Hurricane.

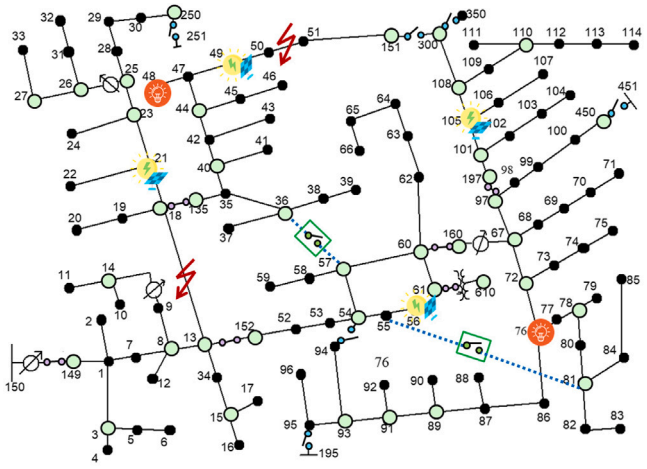

Fig. 24. Contingency IV: Short-circuit event.

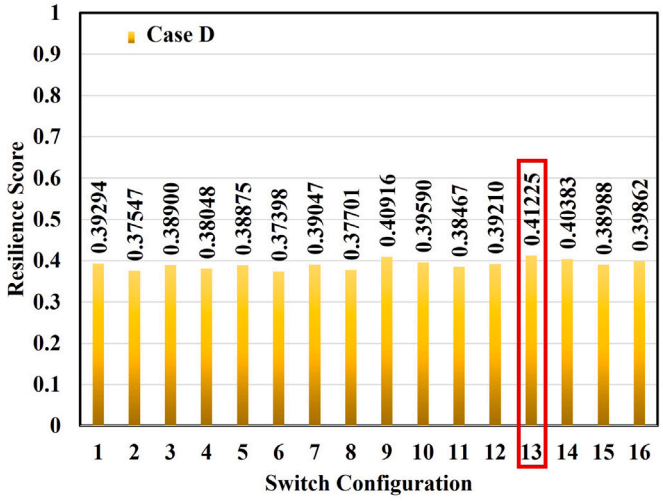

Fig. 25. Resilience scores for possible switches topology during contingency IV: Short-circuit event.

It is observed that under normal operating conditions, resilience is maximum when all switches are closed. However, under extreme events, it is observed that the resilience value is higher for other switch configurations. The same extreme events could occur in the different locations of the EDS, and the resilience of the system could be improved by an assessment of regional vulnerabilities to identify why certain areas were more affected. Also, a strategic placement of DERs would provide alternate paths to meet CLs when other sources are unable to find paths to provide supply to CLs. Smart grid technologies could also be employed to enhance fault detection and facilitate automatic recovery processes. Moreover, the decentralization of power distribution through microgrids and distributed generation could enable parts of the network to remain operational independently during disruptions. Proactive investment in preventive measures, including routine maintenance, will significantly mitigate outage risks. Finally, refining emergency response strategies, regular drills, and clear communication will ensure swift and efficient action during crises, minimizing downtime and expediting service restoration.

It is to be noted that restoration strategies are fundamental to system resilience but are inherently system-specific, varying with operator expertise and available resources. The proposed metric quantifies resilience through electrical service and topological parameters that provide consistent measurement across different systems and operational states. While the metric excludes specific restoration methodologies to maintain standardized assessment capabilities, it enables operators to evaluate restoration effectiveness by comparing resilience scores before and after restoration activities.

The step-by-step decision-making process of the electrical distribution system operator in Fig. 27. The performance of the system is continuously monitored, and the detection of extreme events is checked. Following the detection of such events, the operator needs to isolate the affected areas for the prevention of cascading effects and assess the extent of system degradation. The disruption of service to CLs needs to be checked, and if the load demand is not met, possible switch configurations are checked, and the most resilient configuration is selected. During this time, the operator could complete the repairs to the infrastructure and gradually restore the service to all customers.

6.5. Summary: Alignment of the proposed metric with key enablers of the resilience analysis process

The proposed resilience metric for EDS is designed to provide decision-makers with a comprehensive tool for analyzing both topological characteristics and functional aspects of the network, thereby helping to prioritize improvements and investments. This metric facilitates comparisons across different power distribution systems by incorporating both topological and functional parameters, making it applicable in both operational and planning scenarios. Moreover, the proposed metric is characterized by its adaptability and scalability, allowing it to effectively capture varying timeframes and geographical

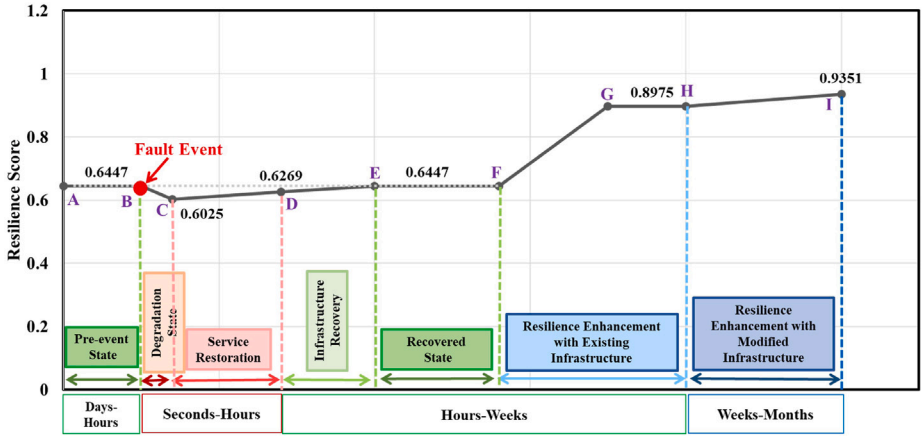

Points	Case Details
A & B	Case A with 4 DERs.
C	Case A with 4 DERs under event conditions.
D	Case D with 4 DERs under event conditions.
E & F	Case A with 4 DERs after recovering from an extreme event.
G & H	Case D with 4 DERs after recovering from an extreme event.
I	Case D with additional switches with 4 DERs after recovering from an extreme event.

Fig. 26. Resilience curve during contingency IV: Short-circuit event.

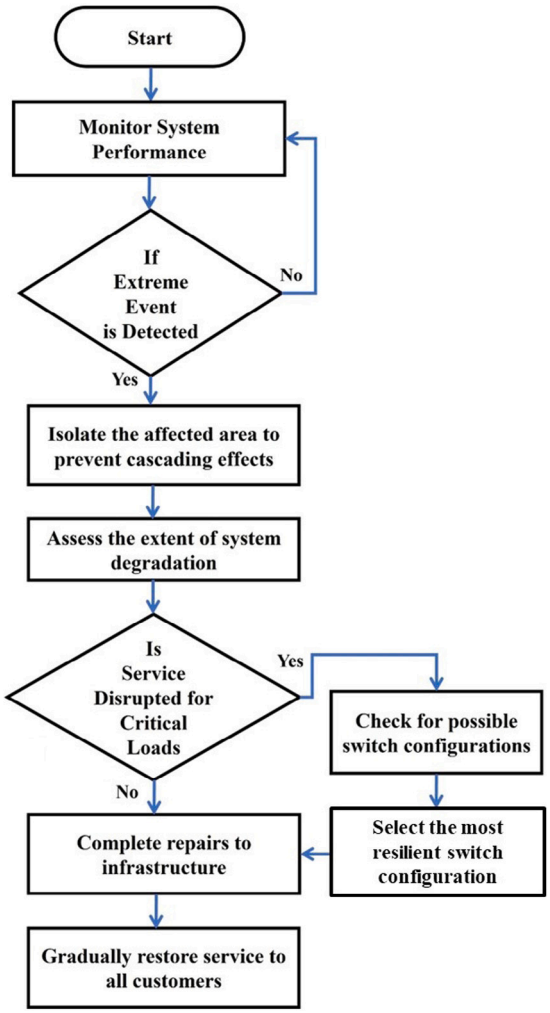

Fig. 27. Decisions to be taken by distribution system operator.

contexts. It combines quantitative measures, such as percolation threshold analysis and the number of critical loads served, with qualitative measures like information centrality, providing a balanced assessment of resilience that accommodates both numerical data and qualitative insights. The inclusion of percolation threshold analysis helps identify critical points in the network, considering uncertainty and the potential for cascading failures, thus offering a more robust resilience assessment. From the resilience curve provided by the proposed metric, decision-makers could gain an understanding of the system's recovery capabilities, which is essential for assessing and improving the recovery time after an outage.

7. Conclusion

This paper presents a comprehensive framework for evaluating and enhancing the resilience of electrical distribution systems, which is increasingly crucial in the face of escalating extreme weather events. The proposed methodology incorporates topology-based and electrical service-based resilience parameters. It offers a quantitative framework for assessing and selecting resilient strategies, including the integration of distributed energy resources and the operation of additional switches. This metric aligns with the established definition of resilience provided by the IEEE task force and incorporates key elements identified by Sandia National Laboratories, ensuring its robustness and applicability.

The proposed resilience metric has been thoroughly evaluated against various contingency events, such as floods, wildfires, hurricanes, and short-circuit faults, with its effectiveness demonstrated on the modified IEEE 123 node test feeder. By integrating both topological and electrical service parameters, the metric provides operators with a comprehensive analysis that supports risk-based decision-making for resilient system operation. Also, the resilience curve visually reinforces the effectiveness of the proposed resilience metric. From the initial pre-event state through fault events and strategic planning, the curve achieves a highly resilient system. This signifies the system's robustness in withstanding and recovering from adverse events.

Furthermore, the paper introduces a systematic approach to enhance resilience through strategic integration of DERs and automated switches into the EDS. The findings affirm the proposed metric as a valuable tool for resilience-based planning, presenting operators with a methodical process to maximize resilience and maintain robust, adaptable, and swift recovery capabilities in the face of adversities. The proposed framework and metric guide future resilience enhancement initiatives and could become integral to the planning and operation of resilient electrical distribution systems. In future works, different parameters that give more insights into the phase transition of the system could be analyzed. Also, AI techniques that provide early detection of the grid instabilities leading to blackouts could also be included in the resilience parameters.

CRediT authorship contribution statement

Divyanshi Dwivedi: Writing – original draft, Visualization, Validation, Software, Methodology, Formal analysis, Data curation. **K. Victor Sam Moses Babu:** Writing – original draft, Visualization, Validation, Software, Methodology, Formal analysis, Data curation. **Pradeep**

Kumar Yemula: Writing – review & editing, Supervision. **Pratyush Chakraborty:** Writing – review & editing, Supervision. **Mayukha Pal:** Writing – review & editing, Validation, Supervision, Software, Resources, Project administration, Methodology, Investigation, Funding acquisition, Conceptualization.

Declaration of competing interest

The authors declare that they have no known competing financial interests or personal relationships that could have appeared to influence the work reported in this paper.

Acknowledgments

Divyanshi Dwivedi and K. Victor Sam Moses Babu would like to thank ABB Ability Innovation Centre, Hyderabad for the financial support in research. The author Mayukha Pal would like to thank the ABB Ability Innovation Center, Hyderabad, for their support in this work.

Data availability

Data will be made available on request.

References

[1] Diahovchenko IM, Kandaperumal G, Srivastava AK, Maslova ZI, Lebedka SM. Resiliency-driven strategies for power distribution system development. Electr Power Syst Res 2021;197:107327.
[2] Dwivedi D, Yemula PK, Pal M. Evaluating the planning and operational resilience of electrical distribution systems with distributed energy resources using complex network theory. Renew Energy Focus 2023;46:156–69.
[3] Blake ES, Kimberlain TB, Berg RJ, Cangialosi JP, Beven Ii JL. Tropical cyclone report: Hurricane sandy. National Hurricane Center 2013;12:1–10.
[4] Administration UEI. U.S. electricity customers experienced eight hours of power interruptions in 2020. 2021, https://www.eia.gov/todayinenergy/detail.php?id=50316.
[5] Shackelford R, Paddison L, Ataman J, Subramaniam T. Storm Ciarán batters Northwest Europe, killing at least 4 people and cutting 1 million off power grids. 2023, https://edition.cnn.com/2023/11/02/weather/storm-ciaran-france-uk-electricity-northwestern-europe-climate-gbr-intl/index.html.
[6] Kaloti SA, Chowdhury BH. Toward reaching a consensus on the concept of power system resilience: Definitions, assessment frameworks, and metrics. IEEE Access 2023;11:81401–18.
[7] NPR. California storms bring more heavy rain, flooding and power outages. 2023, https://www.npr.org/2023/01/14/1149304548/california-storms-flooding-newsom.
[8] Fox L. Heavy rain in ottawa causes flooding, power outages and road closures. 2023, https://globalnews.ca/news/9889120/flooding-power-outages-ottawa/.
[9] Calma J. California's solar energy gains go up in wildfire smoke. The Verge 2020. Science reporter covering the environment, climate, and energy with a decade of experience. Host of the Hell or High Water podcast, https://www.theverge.com/2020/10/1/21496088/california-solar-energy-loss-wildfire-smoke-pollution.
[10] Waseem M, Manshadi SD. Electricity grid resilience amid various natural disasters: Challenges and solutions. The Electricity J 2020;33(10):106864.
[11] Holling CS. Resilience and stability of ecological systems. Ann Rev Ecology Systemat 1973;4(1):1–23.
[12] Lachs WR. Controlling grid integrity after power system emergencies. IEEE Power Eng Rev 2002;22(2):61–2.
[13] Panteli M, Mancarella P. The grid: Stronger, bigger, smarter?: Presenting a conceptual framework of power system resilience. IEEE Power Energy Mag 2015;13(3):58–66.
[14] Microgrids as a resilience resource and strategies used by microgrids for enhancing resilience. Appl Energy 2019;240:56–72.
[15] Stanković AM, Tomsovic KL, De Caro F, Braun M, Chow JH, Čukalevski N, Dobson I, Eto J, Fink B, Hachmann C, Hill D, Ji C, Kavicky JA, Levi V, Liu C-C, Mili L, Moreno R, Panteli M, Petit FD, Sansavini G, Singh C, Srivastava AK, Strunz K, Sun H, Xu Y, Zhao S. Methods for analysis and quantification of power system resilience. IEEE Trans Power Syst 2023;38(5):4774–87.
[16] Diahovchenko IM, Kandaperumal G, Srivastava AK. Enabling resiliency using microgrids with dynamic boundaries. Electr Power Syst Res 2023;221:109460.
[17] Panwar M, Chanda S, Mohanpurkar M, Luo Y, Dias F, Hovsapian R, Srivastava AK. Integration of flow battery for resilience enhancement of advanced distribution grids. Int J Electr Power Energy Syst 2019;109:314–24.
[18] Stanković AM, Tomsovic KL, De Caro F, Braun M, Chow JH, Čukalevski N, Dobson I, Eto J, Fink B, Hachmann C, Hill D, Ji C, Kavicky JA, Levi V, Liu C-C, Mili L, Moreno R, Panteli M, Petit FD, Sansavini G, Singh C, Srivastava AK, Strunz K, Sun H, Xu Y, Zhao S. Methods for analysis and quantification of power system resilience. IEEE Trans Power Syst 2023;38(5):4774–87.
[19] Kandaperumal G, Pandey S, Srivastava A. AWR: Anticipate, withstand, and recover resilience metric for operational and planning decision support in electric distribution system. IEEE Trans Smart Grid 2022;13(1):179–90.
[20] Chanda S, Srivastava AK, Mohanpurkar MU, Hovsapian R. Quantifying power distribution system resiliency using code-based metric. IEEE Trans Ind Appl 2018;54(4):3676–86.
[21] Chanda S, Srivastava AK. Defining and enabling resiliency of electric distribution systems with multiple microgrids. IEEE Trans Smart Grid 2016;7(6):2859–68.
[22] Watson J-P, Guttromson R, Silva-Monroy C, Jeffers R, Jones K, Ellison J, Rath C, Gearhart J, Jones D, Corbet T, Hanley C, Walker LT. Conceptual framework for developing resilience metrics for the electricity, oil, and gas sectors in the United States. 2014.
[23] Fisher RE, Norman M. Developing measurement indices to enhance protection and resilience of critical infrastructure and key resources. J. Bus. Cont Emerg Plan 2010;4(3).
[24] Kwasinski A. Quantitative model and metrics of electrical grids' resilience evaluated at a power distribution level. Energies 2016;9(2).
[25] Bajpai P, Chanda S, Srivastava AK. A novel metric to quantify and enable resilient distribution system using graph theory and choquet integral. IEEE Trans Smart Grid 2018;9(4):2918–29.
[26] Gao H, Chen Y, Xu Y, Liu C-C. Resilience-oriented critical load restoration using microgrids in distribution systems. IEEE Trans Smart Grid 2016;7(6):2837–48.
[27] Moslehi S, Reddy TA. Sustainability of integrated energy systems: A performance-based resilience assessment methodology. Appl Energy 2018;228:487–98.
[28] Pandey S, Chanda S, Srivastava AK, Hovsapian RO. Resiliency-driven proactive distribution system reconfiguration with synchrophasor data. IEEE Trans Power Syst 2020;35(4):2748–58.
[29] Sia J, Jonckheere EA, Shalalfeh L, Bogdan P. Phasor measurement unit change-point detection of frequency hurst exponent anomaly with time-to-event. IEEE Trans Dependable Secure Comput 2024;21(2):819–27.
[30] Sia J, Jonckheere E, Shalalfeh L, Bogdan P. PMU change point detection of imminent voltage collapse and stealthy attacks. In: 2018 IEEE conference on decision and control. CDC, 2018, p. 6812–7.
[31] Mehigan L, Deane J, Gallachóir B, Bertsch V. A review of the role of distributed generation (DG) in future electricity systems. Energy 2018;163:822–36.
[32] Dwivedi D, Mitikiri SB, Babu KVSM, Yemula PK, Srinivas VL, Chakraborty P, Pal M. Technological advancements and innovations in enhancing resilience of electrical distribution systems. Int J Crit Infrastruct Prot 2024;46:100696.
[33] Uniyal A, Sarangi S. Optimal network reconfiguration and DG allocation using adaptive modified whale optimization algorithm considering probabilistic load flow. Electr Power Syst Res 2021;192:106909.
[34] Diahovchenko I, Viacheslav Z. Optimal composition of alternative energy sources to minimize power losses and maximize profits in distribution power network. In: 2020 IEEE 7th international conference on energy smart systems. ESS, 2020, p. 247–52.
[35] Haimes YY. On the definition of resilience in systems. Risk Anal 2009;29(4):498–501.
[36] Naderi E, Seifi H, Sepasian MS. A dynamic approach for distribution system planning considering distributed generation. IEEE Trans Power Deliv 2012;27(3):1313–22.
[37] Arefifar SA, Mohamed YA-RI, EL-Fouly THM. Optimum microgrid design for enhancing reliability and supply-security. IEEE Trans Smart Grid 2013;4(3):1567–75.
[38] Ma L, Tian J, Zhang T, Guo Q, Hu C. Accurate and efficient remaining useful life prediction of batteries enabled by physics-informed machine learning. J Energy Chem 2024;91:512–21.
[39] Hasib SA, Islam S, Ali MF, Sarker SK, Li L, Hasan MM, Saha DK. Enhancing prediction accuracy of remaining useful life in lithium-ion batteries: A deep learning approach with bat optimizer. Future Batteries 2024;2:100003.
[40] Wang S, Fan Y, Jin S, Takyi-Aninakwa P, Fernandez C. Improved anti-noise adaptive long short-term memory neural network modeling for the robust remaining useful life prediction of lithium-ion batteries. Reliab Eng Syst Saf 2023;230:108920.
[41] Wang S, Wu F, Takyi-Aninakwa P, Fernandez C, Stroe D-I, Huang Q. Improved singular filtering-Gaussian process regression-long short-term memory model for whole-life-cycle remaining capacity estimation of lithium-ion batteries adaptive to fast aging and multi-current variations. Energy 2023;284:128677.
[42] Chuangpishit S, Katiraei F, Chalamala B, Novosel D. Mobile energy storage systems: A grid-edge technology to enhance reliability and resilience. IEEE Power Energy Mag 2023;21(2):97–105.
[43] Prabawa P, Choi D-H. Multi-agent framework for service restoration in distribution systems with distributed generators and static/mobile energy storage systems. IEEE Access 2020;8:51736–52.
[44] Heidari A, Agelidis VG, Kia M. Considerations of sectionalizing switches in distribution networks with distributed generation. IEEE Trans Power Deliv 2015;30(3):1401–9.

[45] Celli G, Pilo F. Optimal sectionalizing switches allocation in distribution networks. IEEE Trans Power Deliv 1999;14(3):1167–72.
[46] Schneider KP, Mather BA, Pal BC, Ten CW, Shirek GJ, Zhu H, Fuller JC, Pereira JLR, Ochoa LF, de Araujo LR, Dugan RC, Matthias S, Paudyal S, McDermott TE, Kersting W. Analytic considerations and design basis for the IEEE distribution test feeders. IEEE Trans Power Syst 2017;PP(99). 1.
[47] Jae N. Percolation transition in networks with degree-degree correlation. Phys. Rev E 2007.
[48] Moore TJ, Cho J-H. Applying percolation theory. In: Kott A, Linkov I, editors. Cyber resilience of systems and networks. Cham: Springer International Publishing; 2019, p. 107–33.
[49] Massaro E, Bagnoli F. Epidemic spreading and risk perception in multiplex networks: A self-organized percolation method. Phys Rev E 2014;90:052817.
[50] Artime O, Grassia M, De Domenico M, et al. Robustness and resilience of complex networks. Nat Rev Phys 2024;6:114–31.
[51] Moore TJ, Cho J-H. Applying percolation theory. In: Kott A, Linkov I, editors. Cyber resilience of systems and networks. Cham: Springer International Publishing; 2019, p. 107–33.
[52] Forero-Sandoval IY, Franco-Bacca AP, Cervantes-Álvarez F, Gómez-Heredia CL, Ramírez-Rincón JA, Ordonez-Miranda J, Alvarado-Gil JJ. Electrical and thermal percolation in two-phase materials: A perspective. J Appl Phys 2022;131(23):230901.
[53] Kranthi T, Rao SB, Manimaran P. Identification of synthetic lethal pairs in biological systems through network information centrality. Mol. BioSyst. 2013;9:2163–7.
[54] López JC, Franco JF, Rider MJ. Optimisation-based switch allocation to improve energy losses and service restoration in radial electrical distribution systems. IET Generat, Transmiss Distrib 2016;10(11):2792–801.
[55] Souto L, Yip J, Wu W-Y, Austgen B, Kutanoglu E, Hasenbein J, Yang Z-L, King CW, Santoso S. Power system resilience to floods: Modeling, impact assessment, and mid-term mitigation strategies. Int J Electr Power Energy Syst 2022;135:107545.
[56] Nazemi M, Dehghanian P. Powering through wildfires: An integrated solution for enhanced safety and resilience in power grids. IEEE Trans Ind Appl 2022;58(3):4192–202.
[57] Bandara S, Rajeev P, Gad E. Power distribution system faults and wildfires: Mechanisms and prevention. Forests 2023;14(6).
[58] Abdelmalak M, Benidris M. Enhancing power system operational resilience against wildfires. IEEE Trans Ind Appl 2022;58(2):1611–21.
[59] Shi Q, Liu W, Zeng B, Hui H, Li F. Enhancing distribution system resilience against extreme weather events: Concept review, algorithm summary, and future vision. Int J Electr Power Energy Syst 2022;138:107860.